INORGANIC CHEMISTRY FRONTIERS

CCS 中国化学会 CHINESE CHEMICAL SOCIETY

ROYAL SOCIETY OF CHEMISTRY

Molecular inspired electrocatalyst materials for environmental remediation

Journal:	*Inorganic Chemistry Frontiers*
Manuscript ID	QI-REV-07-2023-001248.R1
Article Type:	Review Article
Date Submitted by the Author:	15-Aug-2023
Complete List of Authors:	Calvillo Solis, Jonathan ; The University of Texas at El Paso, Department of Chemistry Castillo, Alexandria; The University of Texas at El Paso, Department of Chemistry Yin, Sheng; The University of Texas at El Paso, Department of Chemistry Sandoval Pauker, Christian; University of Texas at El Paso University Research Institute, Department of Chemistry and Biochemistry Ocuane, Neidy; The University of Texas at El Paso, Department of Chemistry Puerto-Diaz, Diego; The University of Texas at El Paso, Department of Chemistry Jafari, Nasim; The University of Texas at El Paso, Department of Chemistry Villagran, Dino; The University of Texas at El Paso, Department of Chemistry

REVIEW

Molecular inspired electrocatalyst materials for environmental remediation

Received 00th January 20xx,
Accepted 00th January 20xx

DOI: 10.1039/x0xx00000x

Jonathan J. Calvillo Solis,[a,b] Alexandria Castillo,[a,b] Sheng Yin,[a,b] Christian Sandoval-Pauker,[a,b] Neidy Ocuane,[a,b] Diego Puerto-Diaz,[a,b] Nasim Jafari,[a] Dino Villagrán*[a,b]

The increasing presence of chemical contaminants in the environment due to demands associated with a growing population and industrial development poses risks to human health due to their exposure. Electrochemical degradation has emerged as a promising remediation technology for environmentally relevant pollutants. This review evaluates the advances in the application of molecularly-inspired catalysts for the electrochemical degradation of nitrate/nitrite, halogenated compounds, aromatic hydrocarbons, and pharmaceuticals. The impact of molecular structure composition on electrochemical parameters such as conversion rates, selectivity, and Faradic efficiency is described. The potential applications of electrochemical degradation for poly- and per-fluoroalkyl substances are briefly mentioned. The utilization of computational chemistry in investigating catalytic sites, reaction mechanisms, and electronic structure is also discussed. This review contributes to understanding molecular-inspired electrocatalysts for the degradation of major environmental pollutants.

1. Introduction

Since 1950, the rapid population and industrialization growth have required the increased use of chemical products to meet the high demands in agriculture, pharmaceutical, food, and manufacturing industries, among others.[1] However, the consequences to the environment have been significant by the presence of hazardous substances. Aromatic hydrocarbons, halogenated molecules, nitrate/nitrite, and poly- and perfluoroalkyl substances (PFAS) are pollutants of priority concern due to their health effects in humans and living organisms (Scheme 1).[2–5] Despite governmental regulations to reduce the environmental impact of the emission of hazardous waste, studies show an increasing environmental presence of these pollutants.[6–8]

Most research has focused on the removal of persistent organic pollutants (POPs) and inorganic species (such as NO_3^-/NO_2^-) from water because they cannot be easily hydrolyzed, photolyzed, or degraded by conventional water treatment methods.[7] Micro-filtration, chemical-photochemical oxidation, adsorption, and biodegradation have resulted in a slow and low removal efficiency on water cleaning systems and wastewater treatment plants.[9] For this reason, more efficient, cheaper, and straightforward methods are necessary to destroy these contaminants and provide clean water access. Progress over the past decades has been made in the application of electrochemical methods for the electrodegradation of pollutants.[10,11] Electrochemical methods can be cheap, easy to implement, provide high removal efficiencies, and have the capability to be powered by renewable electricity, making them environmentally friendly and scalable.[12–14] Most electrochemical processes use anodes and cathodes made of metals, alloys, metallic nanoparticles, metallic foams, metal-carbon scaffolds, and, more recently, boron-doped diamond (BDD),[15] to oxidize or reduce pollutants in water.[16] These materials can promote C–H bond activation,[17] C-C bond homolytic cleavage,[18] decarboxylation reactions,[19] dehalogenation reactions,[20] and other small molecule activation.[21] However, the main issue with metal electrodes is their high cost and their activity towards competitive side reactions such as hydrogen and oxygen evolution (HER and OER, respectively), which drastically limits their efficiency.[22]

Most heterogeneous catalysts are based on metallic or semiconductor surfaces where the active sites are the facets exposed to the substrate. Yet, recent work on electrocatalysts where a molecular node can be identified as the active site has been an area of interest for many research groups. Homogenous catalysis has

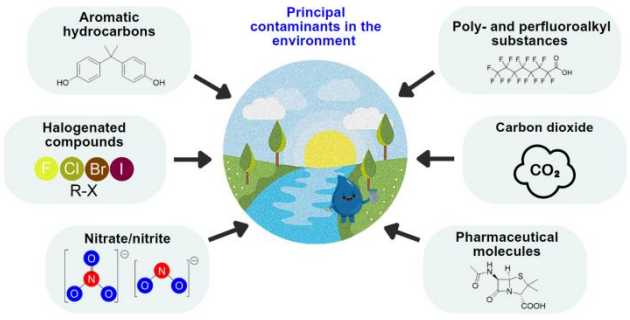

Scheme 1 Pollutants of major public concern in the environment.

[a] Department of Chemistry and Biochemistry, University of Texas at El Paso, 500 W. University Avenue, El Paso, Texas 79968 United States.
[b] Nanosystems Engineering Research Center for Nanotechnology-Enabled Water Treatment (NEWT), USA

been an area of extensive research, since the molecular node can in theory be tuned and analyzed using standard analytical techniques. Recently the use of molecular systems that have been incorporated into polymeric or extended network systems and used as electrocatalysts have gained interest due to the enhanced stability and often enhanced activity of the heterogeneous material. Molecular complexes such as phthalocyanines (Pc),[23] porphyrins (Por),[24] coordination compounds,[25] and molecular based extended networks such as metal-organic frameworks (MOFs),[26] are attractive redox systems due to their potential for ligand modification, structural flexibility, and the ability to incorporate metals, enabling tunability.[27,28] Moreover, the reactivity of molecular inspired electrocatalysts is strongly influenced by the ligand type, including tetrapyrrole, salen, ethylenediamine, polypyridyl, amine groups, aromatic rings, among others.[29] Interestingly, molecular-based electrocatalysts offer a unique advantage in providing insight into the catalytic mechanism, as the metal site within the molecular system is presumed to be the active site. In this review, we aim to provide a summary of recent developments in molecular-inspired electrocatalysts for the degradation of aromatic hydrocarbons, halogenated compounds, nitrate/nitrite, poly- and perfluoroalkyl substances (PFAS). Our focus is to delve into the redox chemistry and mechanistic aspects of each pollutant using electrochemical techniques and provide general working principles of molecular electrocatalysts. Furthermore, we discuss computational approaches as valuable tools for obtaining thermodynamic and mechanistic information pertaining to the electrocatalytic pathways of various heterogeneous molecular catalysts.

2. Degradation of pollutants by molecular inspired electrocatalysts

2.1. Nitrate/Nitrite reduction

Nitrate pollution in ground and surface water as a result of anthropogenic activities has dramatically increased in the past few decades.[30–32] Nitrate in drinking water can detrimentally impact human health by causing methemoglobinemia in newborns and infants, thyroid disease, and increase the risk of cancers.[33–35] The World Health Organization (WHO) has set a maximum contaminant level (MCL) of 50 mg L^{-1} NO_3^- in drinking water, and the Environmental Protection Agency (EPA) has followed suit.[36,37] Electrochemical nitrate reduction (ENR) was first introduced as a means to treat alkaline and nuclear waste solutions in the late 1980s and 1990s, respectively.[38–42] ENR has recently been used to treat waste brines, wastewater, and drinking water.[43–47] Nitrate reduction to ammonia or nitrogen gas (the two most thermodynamically stable nitrogen species) are multi-electron processes as seen in equations 1 and 2. The numerous byproducts and intermediates involved are generally omitted when describing these complex processes.[48]

$$NO_3^- + 9H^+ + 8e^- \rightleftarrows NH_3 + 3H_2O \quad E^o = 1.17 \text{ V vs. SHE} \tag{1}$$

$$2NO_3^- + 12H^+ + 10e^- \rightleftarrows N_2 + 6H_2O \quad E^o = -0.12 \text{ V vs. SHE} \tag{2}$$

The rate-determining step involves the reduction of NO_3^- to NO_2^- as shown in equation 3. Experimentally, this reaction requires an overpotential (η) which is an electrochemical potential that is more negative than the thermodynamic standard value (E° = 0.01 V vs. SHE). The choice of electrode material determines the thermodynamic feasibility and kinetic efficiency.

$$NO_3^- + 2H^+ + 2e^- \rightleftarrows NO_2^- + H_2O \quad E^o = 0.01 \text{ V vs. SHE} \tag{3}$$

The metal coordination complexes that are present in the active sites of these enzymes (e.g., molybdenum-containing nitrate reductase, copper-containing nitrite reductase, etc.) are responsible for such transformations.[49] The elucidation of the active site structures has led to the development of bio-inspired catalysts for the reduction of several nitrogen oxides.[50–56] During nitrate reduction, pH impacts Faradaic efficiency and the product selectivity.[48] In alkaline conditions, the ENR frequently yields nitrite from nitrate,[57] while in acid media, cathodic reduction produces N_2, N_2O, and ammonia in addition to nitrite.[58] However, enhancing conversion yields in acid media as a function of voltage results in competing side reactions such as hydrogen evolution (HER). As shown in equations 1-3, H^+ are consumed in all electrochemical transformations, which makes charge transfer kinetically unfavorable at pH ~ 7.[59] In unbuffered solutions, the pH increases during the bulk electrolysis, which limits the H^+ availability. Flow systems compensate for the pH variations during electrolysis and the design molecular systems that can selectively reduce nitrate even in acidic conditions.

Molecular inspired electrocatalysts have been explored as promising materials for NO_3^- and NO_2^- transformation,[60–66] and Table 1 shows representative examples for nitrate reduction and their corresponding metrics and parameters. An early report has shown that Co(III)-cyclam and Ni(II)-cyclam on mercury electrodes show preference for hydroxylamine production, and preference for ammonia at silver, copper, and lead electrodes with similar results for nitrite conversion.[62] A water-soluble iron porphyrin $[Fe(H_2O)(TPPS)]^{3-}$ (H_2TPPS^{4-} = tetraanonic form of *meso*-tetrakis(*p*-sulfonatophenyl)porphyrin),[61] electrochemically converts nitrate to ammonia with a 26–49% conversion efficiency at pH 4.5, with a cathodic potential of –0.9 V vs. SHE, applying a current density (*j*) of 8.3 mA cm^{-2}. At pH 6.7, ammonia production is favored with a conversion yield of 82–97%, at the same potential and *j* of 1.5 mA cm^{-2}. Nickel, lead, zinc, and iron cathodes coated with a Fe-phthalocyanine (Pc) molecular catalyst show enhanced electrochemical activity versus bare metal cathodes in alkaline media with 71% ammonia conversion with the Pc/Fe electrode.[63]

Recent studies have investigated the role of proton shuttles present in macrocyclic ligands.[67] A cobalt complex with a DIM (2,3-dimethyl-1,4,8,11-tetraazacyclotetradeca-1,3-diene) macrocyclic ligand produces ammonia as the sole product from NO_3^- and NO_2^- in unbuffered aqueous solutions.[68,69] The protonation of nitrate/nitrite and the N–O bond cleavage step are facilitated by both the redox active diimine moiety and amine proton shuttles present in the DIM

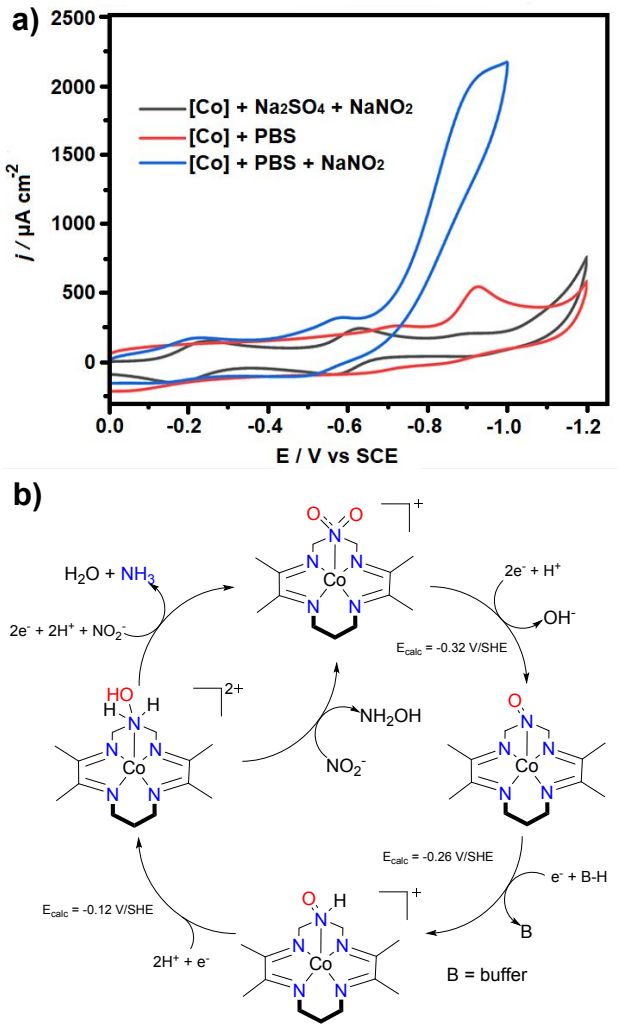

Fig. 1 Electrocatalytic nitrite reduction enhanced by presence of PBS at pH 7. (a) Cyclic voltammogram of 0.5 mM $[Co(TIM)Br_2]^+$ in different conditions, in presence of 20 mM $NaNO_2$ and 0.1 M Na_2SO_4 (black), with 0.1 M PBS (red) and 20 mM $NaNO_2$ and 0.1 M PBS (blue), v = 200 mV s^{-1}. (b) Proposed electrocatalytic mechanism. Reproduced with permission from ref. 72. Copyright © 2022. American Chemical Society.

ligand.[70] Whereas $[Co(cyclam)Cl_2]^+$ (cyclam = 1,4,8,11-tetraazacyclotetradecane) and $[Co(TIM)Br_2]^+$ (TIM = 2,4,9,10-tetramethyl-1,4,8,11-tetraazacycldec-1,3,8,10-tetraene), are inactive due to the lack of amine proton shuttles.[71] However, in the presence of a phosphate buffer solution (PBS), $[Co(TIM)Br_2]^+$ can reduce nitrite to ammonia with the buffer acting as a proton shuttle, as shown in the voltammetric response (Fig. 1a) and the proposed mechanism (Fig. 1b).[72] The catalytic activity of complexes with the same metal center can be determined by investigating structurally similar molecules and elucidating the properties provided by the supporting macrocyclic ligands, thus, facilitating the rational design of molecular catalysts for nitrate/nitrate reduction.

Carbonaceous supports such as glassy carbon[60,73–76], graphite,[77,78] and carbon nanotubes[79–81] have been utilized to enhance the electrochemical performance and stability of metal-based catalysts. Cobalt and copper phthalocyanines (CoPc, CuPc) anchored on carbon nanotubes electrochemically convert nitrate to ammonia with higher activity and selectivity than aggregated Pc samples.[79–81] The CNT-supported CuPc material is 30% more active than the carbon black-supported CuPc.[79] CuPc requires a lower NO_3^- reduction overpotential (η) compared to the cobalt analog to reach a *j* of 10 mA cm^{-2} and a Faradaic efficiency (FE) over 98%. NiPc-CNT sponges achieve 98% nitrate removal after 4h of electrolysis due to the high electrochemically active surface (ECSA) layer of the CNT sponge.[80] CoPc has the overall highest performance for nitrate reduction, with an ammonia conversion rate > 97%.[81] A family of $Co(dmgH_2)Cl_2$ (dmg = dimethylglyoximato) immobilized on multiwalled CNTs (MWCNT) show a 5-fold increase in current density compared to bare MWCNTs in the nitrite to ammonia electrochemical conversion with FE of 86–98% and preference to ammonia.[82] Pyridine-based axial ligands increase intramolecular hydrogen bonds and proton shuttles, and fused diamine-dioximine groups add structural stability. $[Co(DIM)Br_2]^+$ and $[Fe(DIM)Cl_2]^+$ immobilized on oxidized glassy carbon electrodes (GCE)[73,74] enhances the nitrite and nitrate reduction kinetics due to the incorporation to the modified GCE. A FE of 98.5% for nitrite reduction to ammonium is observed for the $[Co(DIM)Cl_2]^+$ modified GCE at –1.16 V vs. SHE. Similarly, $[Fe(DIM)Cl_2]^+$ has a FE of 88% for nitrate reduction to ammonia at –0.86 V vs. SHE. Metal proto-porphyrins (M-PP) (i.e., Co(III), Fe(II), Ni(II), Cu(II), Rh(II)) adsorbed onto pyrolytic graphite show enhanced reactivity towards hydroxylamine and ammonia formation in acidic media.[77] At acidic pH values, hydroxylamine is the main product at 100% selectivity with the Co-PP system.

Metal organic frameworks (MOFs) have also been utilized for nitrate reduction attention due to their porous structures and unsaturated metal sites, especially those derived from conjugated organic moieties, which increase conductivity.[83] A heterobimetallic Cu/Co MOF used for nitrate reduction to ammonia achieves a FE of 96% at −0.6 V vs. SHE.[84] Similar findings (i.e. FE of 99% at −0.3V vs. SHE) are reported for a $Cu/CuO_2/CuO$ heterostructure derived from a Cu MOF.[85] Cu^{II}-bipyridine-based thorium MOF (Cu@Th-BPYDC) utilized for ammonia storage upon electroreduction of nitrate with a FE = 92% and storage of 20.55 mmol g^{-1} of NH_3 at standard pressure and temperature.[86] The *in situ* formation of Cu nanoclusters (4 nm) on a MOF after metal ion deposition[87] leads to a uniform distribution of Cu active sites inside the MOF, and it achieves 93% ammonia selectivity and FE of 85% at −0.9 V vs. SHE. A Fe/Ni dual atom MOF exhibits 98% nitrate conversion in 30 minutes with 99% selectivity for nitrogen gas.[88] While the Fe sites lower the energy barrier for nitrate reduction, the Ni sites enhance the adsorption of reaction intermediates. Ni-based MOF nanosheets exhibit 97% nitrate conversion with 80% ammonia selectivity.[89]. Increased ammonium selectivity (100%) at −1.50 V vs. SHE is obtained for a Ni-MOF supported on Ru_xO_y clusters.[90] Palladium metals nanodots incorporated into the pores of a redox-active Zr-MOF tethered by tetrathiafulvalene linkers show a FE of 58% for nitrate reduction to ammonia, while silver and gold nanodots have lower efficiencies.[91]

2.2. Halogenated compounds

Halogenated organic compounds (HOCs) are molecules in which at least one halogen atom (F, Cl, Br, or I) is linked in a carbon chain.

HOCs are employed in refrigerants, solvents, flame-retardants and pesticides, as well as dry cleaning liquids, and as precursors in organic synthesis.[92] Polychlorinated dibenzo-*p*-dioxins, polychlorinated biphenyls (PCBs), hydrochlorofluorocarbons, polychloromethanes, and 1,2-dichloroethane are HOCs of human health concern since they can be easily stored in fatty tissues and lead to hormonal disruption, neurotoxic damage, teratogenesis, mutagenesis, and cancer.[93,94] Since the 1990s HOCs have been categorized as persistent organic pollutants by the United Nations Environment Program.[95] In 2004, many HOCs were banned under the Stockholm Convention. For example, dichlorodiphenyltrichloroethane (DDT), one of the most controversial pesticides, was globally banned and is currently only used in a few South Asian countries.[96] Thus, the removal of HOCs from waterbodies is essential in global water treatment. HOCs are treated by chemical reduction processes to remove halides from the alkyl chains, as shown in equation 4.[97]

$$R\text{-}X + H_2 \xrightarrow{\text{Catalyst}} R\text{-}H + H\text{-}X \quad (4)$$

Chemical dehalogenation involves using hydrogen gas and often a precious group metal such as Au, Ag, Pt, and Pd.[98] Although this method is generally efficient,[21] it can be expensive since it requires a constant supply of hydrogen gas (which needs to be carefully controlled), and it is not generally applicable to trace amounts of pollutants.[99] Thermal decomposition is an alternative method for HOC removal but requires high temperatures and can result in the formation of toxic byproducts such as halide oxides,[100] and microbiological and enzymatic degradation processes are time-consuming, expensive, and have low conversion yields.[20,101] Electrochemical dehalogenation[12,97,102] requires heterogenous electrodes typically made of expensive Ag and Pd (since they can easily adsorb hydrogen) to catalyze the X/H exchange,[103,104] and their surface can easily be passivated during the initial electrolysis steps.[105] Molecular inspired electrocatalysts can be efficient and affordable options for dehalogenation of HOCs, and Table 1 shows some representative examples and their corresponding metrics and parameters. The dehalogenation of dichloromethane (CH_2Cl_2) in aqueous via dropcasted Cu(I) di-triazole (CuT2) molecular electrocatalyst can be performed with a *j* of −25.1 mA cm^{-2} at −1.4 V vs. SHE. The linear sweep voltammetry shows a significant increase in the current density (Fig. 2a), showing the electrocatalytic capacity of CuT2 in the presence of CH_2Cl_2. CuT2 reveals a preference for producing methane with a FE of 70% and the production of ethane and ethylene byproducts. DFT simulations (*vide infra*) show that the Cu(I) center coordinates CH_2Cl_2 and promotes the C−Cl bond dissociation and protonation, as shown in the proposed mechanism described in Fig. 2b.[25] A metal free triazole-porphyrin (H2PorT8) can electrochemically reduce CH_2Cl_2 to CH_4 in acetonitrile as a solvent, with a FE of 70 % and *j* of −13 mA cm^{-2} at a potential of −1.56 V vs. SHE. The metal-free porphyrin center is the active site, and after a one electron reduction, an N-CH_2Cl radical intermediate is formed, which can be further reduced in two steps to CH_4.[106]

A similar contaminant, 1,2-dichloroethane can be electrodegraded to ethane (100% removal efficiency) with a cobalt phthalocyanine molecular scaffold supported on multiwalled carbon nanotubes (CoPc/CNT). The high efficiency is attributed to the HER suppression and the selectivity of the active center for C-Cl bond breaking, which is considered the rate-determining step.[22] Binuclear iron phthalocyanine (bi-FePc) complexes lead to the dichlorination of atrazine, a commercial herbicide, during 48 h electrolysis with a removal efficiency of 98.2% at a potential of 0.09 V vs. SHE. The electrocatalytic process is favored by the strong adsorption of atrazine on the bi-FePc surface, and the electrochemical production of OH^- ions promote the exchange of chloride.[107] Chloroacetanilide-based herbicides are widely used in agriculture, and one of the most important is alachlor, 2-Chloro-*N*-(2,6-diethylphenyl)-*N*-(methoxymethyl)acetamide, which can be electrodegraded by a cobalt porphyrin complex composed of eight-triazole unites

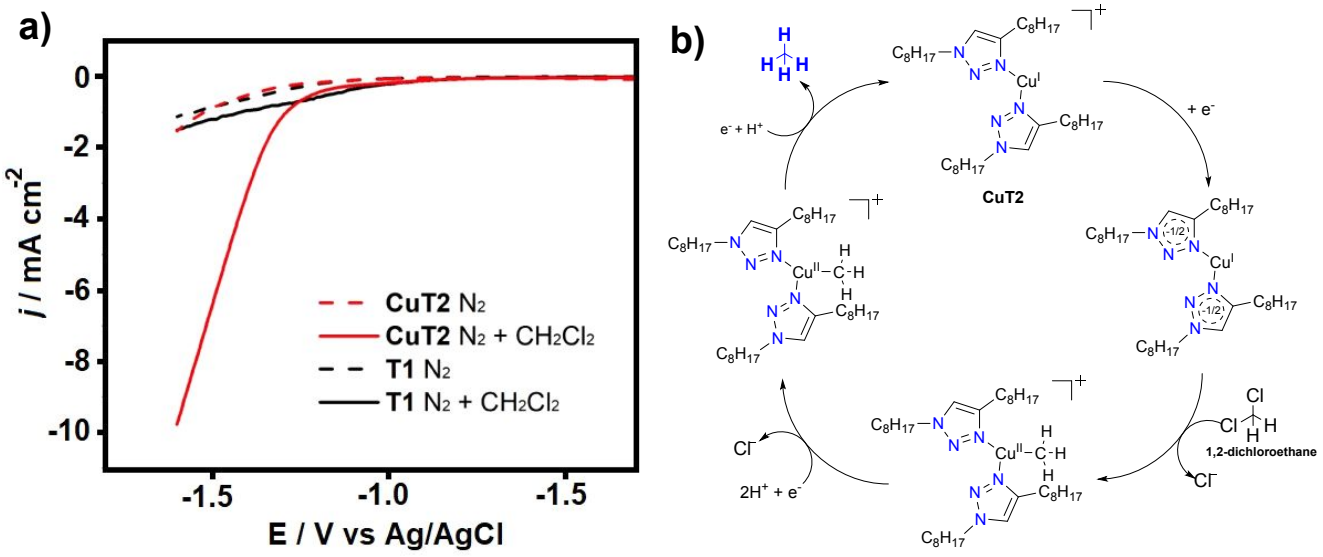

Fig. 2 (a) Linear sweep voltammetry of CuT2 (dashed red line) and the copper-free triazole unit T1 (dashed black line) under nitrogen atmosphere, and CuT2 (solid red line) and T1 (solid black line) with CH_2Cl_2, v = 10 mV s^{-1}. (b) Proposed catalytic route to produce CH_4 as of CH_2Cl_2 using CuT2. Reproduced with permission from ref. 25. Copyright © 2021. American Chemical Society.

(CoPor8T). A conversion yield of 84% was reported at −1.16 V vs. SHE at a *j* of −4.8 mA cm^{-2}. Reduction of Co(II) to Co(I) is followed by a ligand-centered reduction that promotes chloride elimination and oxidative addition of the dehalogenated ligand to the reactive Co(I) center, which is eliminated after a two electron reduction.[29] Similarly, an electrografted $[Co(bpy(CH_2OH)_2)_2]^{2+}$ complex can remove alachlor at −1 V vs. SHE with a removal efficiency of 95% after 40 min of electrolysis. Total organic carbon (TOC) measurements show the selective dechlorination reaction of alachlor in the presence of other chlorinated species.[108] Cobalamin, or Vitamin B12 (VB12), can be used for the dechlorination of trichloroacetic acid to produce acetic acid in a 93% at a *j* of −7 mA cm^{-2} under 5 h, with dichloroacetic acid and monochloroacetic acid as minor byproducts.[109] Similarly, VB12 can also debrominate tribromoacetic acid with 99% of FE after 6h under optimal galvanostatic conditions (*j* = −10.0 mA cm^{-2}). *In situ* Raman spectroscopy shows Co–Br bond formation, which significantly enhances the electron transfer due to is the main step to initiate the debromination process.[110]

2.3. Aromatic hydrocarbons

Aromatic hydrocarbons have one or more conjugated planar rings of π-bonds, which allows for the delocalization of electrons resulting in increased chemical and thermal stability.[111, 112] Aromatic compounds are important units for synthesizing commodity chemicals such as polyaromatic hydrocarbons (PAHs), dyes, fuels, detergents, pesticides, and pharmaceuticals with wide applications.[113,114] However, some of these compounds have toxic and carcinogenic effects,[115] be prone to bioaccumulation, and cause teratogenic effects and genetic mutations.[116] In the environment, aromatic hydrocarbons are often found in wastewaters and soil due to their amphoteric properties,[117] and some of them (e.g., PAHs) are not completely removed by water treatment plants and modern filtration systems.[114] Advanced oxidation processes can only partially degrade them, producing shorter chains with similar toxicologic issues.[118]

The degradation of aromatic pollutants by electrochemical methods using molecularly-inspired catalysts has recently attracted attention.[119,120] For instance, γ-hexachlorocyclohexane, commercially named Lindane, is an organochlorine pesticide, historically widely utilized in agriculture and now known to have serious environmental concerns. Lindane is a persistent pollutant found in surface waters, groundwaters, and soils.[121] An iron based ZSM-zeolite, Fe-ZSM-5, has been employed as a galvanostatic electrocatalyst for Lindane degradation at potentials necessary to maintain a *j* of 30 mA cm^{-2} for 8 h with a removal efficiency of 78%. The electrochemical degradation of Lindane happens through hydrogen free radicals (H*) produced by the cathodic reduction of H^+ ions and followed by •OH oxidation that results in ring opening.[122] The electrochemical reduction of nitrobenzene can be performed using a covalent triazine framework based on 1,4-phenylenediamine (PD-CTF) to yield phenylhydroxylamine.[123] The electrodegradation of phenol to CO_2 and H_2O occurs on molybdenum disulfide nanosheets composited on ZIF-8-derived nitrogen-doped dodecahedral carbon (MoS_2@ZNC). Electrochemical analyses show an enhancement of the

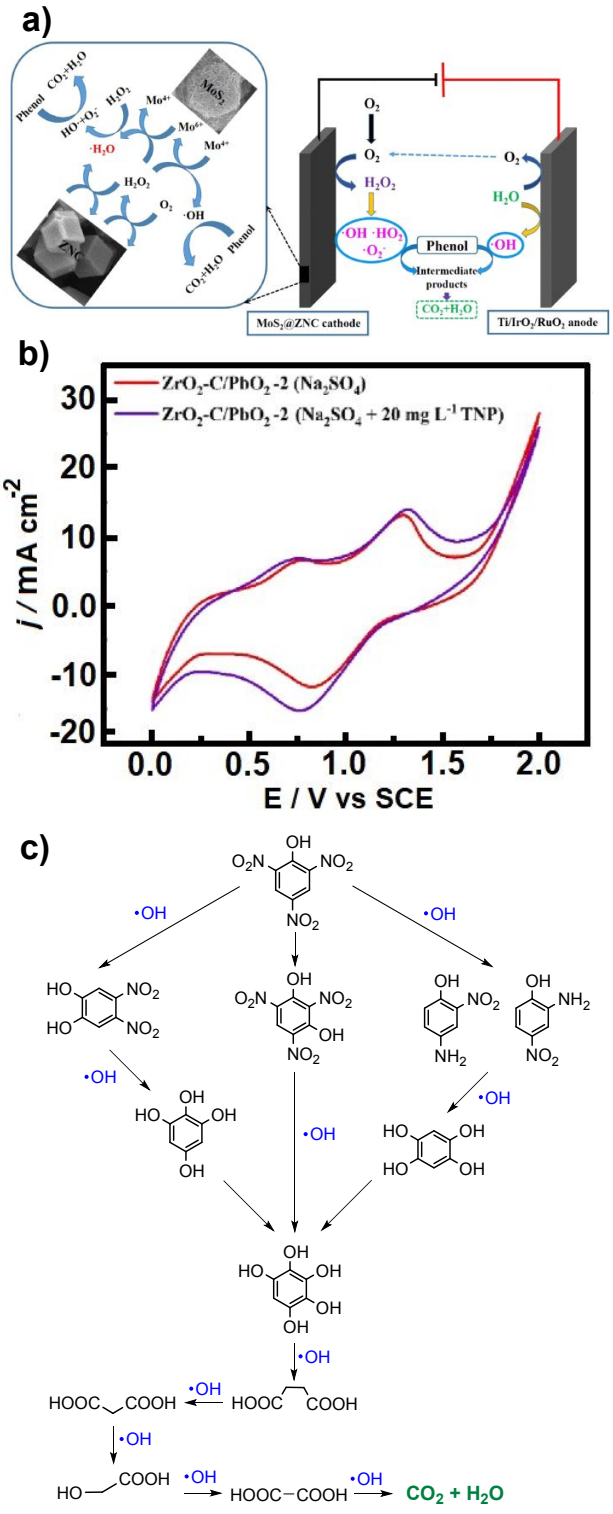

Fig. 3 (a) Schematic diagram for the electrodegradation of phenol by MoS_2@ZNC cathode. Reproduced with permission from ref. 124. Copyright © 2022, Elsevier. (b) Cyclic voltammogram of ZrO_2-C/PbO_2-2 in 20 mg L^{-1} trinitrophenol (TNP) + 0.1 M Na_2SO_4, v = 100 mV s^{-1}. (c) Proposed mechanism for the electrodegradation of TNP with a ZrO_2-C/PbO_2-2 electrode. Reproduced with permission from ref. 125. Copyright © 2023, Elsevier.

electrochemical activity of ZNC by the addition of MoS_2. A phenol removal efficiency of 98.8% was achieved by applying a *j* of 30 mA cm^{-2} for 2h. The high efficiency at alkaline conditions is due to

electrochemical hydrogen peroxide conversion to •OH and $•O_2^-$ radicals (equations 5 and 6):

$$H_2O_2 + OH^- \rightarrow HO_2^- + H_2O \quad (5)$$

$$H_2O_2 + HO_2^- \rightarrow •OH + •O_2^- + H_2O \quad (6)$$

These oxygen-reactive species have a higher oxidation capacity, which allow phenol to be more efficiently degraded into CO_2 and H_2O (Figure 3a). [124] UiO-66-derived ZrO_2-C deposited on a PbO_2 electrode has been used for the anodic oxidization of 2,4,6-trinitrophenol (TNP) to CO_2 and H_2O. The electrochemical characterization by cyclic voltammetry (Figure 3b) shows an increment in the peak current for the ZrO_2-C/PbO_2 electrode due to more accessible active sites and enhanced electron transfer. The composite improves the removal efficiency of TNP when compared to bare PbO_2 anodes (95 vs. 68%) at *j* of 60 mA cm^{-2} for 2.2 h, with a TNP initial concentration of 20 mg L^{-1}. Figure 3c shows a possible degradation pathway of TNP, hydroxyl radicals electrogenerated perform the complete denitrification. Eventually, a ring-opening reaction in the benzene ring may occur to generate intermediates of carboxylic acids which could be further oxidized to CO_2 and H_2O.[125]

Large biomolecular systems, such as deoxyribonucleic acid (DNA) can be used as a scaffold for electrocatalytic materials. For instance, Cobalt Tungsten Oxide Hydroxide Hydrate (CTOHH) deposited on DNA allows for the dispersion of CTOHH over chains of 110 ± 15 nm diameter to avoid aggregation. High temperature annealing of CTOHH-DNA and CTOHH into $CoWO_4$-DNA and $CoWO_4$ at a temperature of 600 °C, yield electrocatalytic materials that can be used for the oxidation of aromatic alcohols. CTOHH-DNA can degrade methoxybenzyl alcohol with an efficiency of 91% in 24 hours at 110 °C which shows that DNA scaffolds can be used to disperse heterogeneous metal nanoparticles to enhance their efficiency.[126]

2.4. Pharmaceuticals molecules

Pharmaceuticals are compounds used for medical or health-related purposes, such as antibiotics, analgesics, anti-inflammatories, hormones, and more.[127] Their impact on human development and their widespread use have environmental drawbacks since their residual presence in water bodies and soil is a current global concern.[128,129] Among the most concerning pharmaceutical pollutants are those whose degradation is slower and those whose activity can directly affect wildlife and plants, and examples of these are non-steroidal anti-inflammatory drugs, antibiotics, beta-blockers (β-blockers), antiepileptic drugs, and blood lipid-lowering agents, antidepressants, hormones, antihistamines, and x-ray contrast media.[130]

Traditional treatment methods, such as those found in wastewater treatment plants, can often not completely remove pharmaceutical contaminants.[131] For instance, the removal efficiency of some pharmaceutical compounds by water treatment systems can be as low as 10%.[132] Pharmaceutical traces are typically detected at low concentrations, ranging from micrograms per liter (μg L^{-1}) to nanograms per liter (ng L^{-1}). [133–135] Even at these low levels, they can still have adverse environmental effects.[136] In this context, it is necessary to develop materials and techniques to degrade pharmaceutical wastes properly before they enter the environment.[137] The Electro-Fenton (EF) method has been gaining attention as an alternative water treatment process. As shown in equation 7, EF relies on the *in situ* electrochemical generation of H_2O_2 at the cathode by a two-electron oxygen reduction reaction which avoids reagent storage and transportation, which diminishes their associated risks. Fe(II) ions are then oxidized to produce hydroxyl radicals, as is shown in equation 8.[138]

$$O_2 + 2H^+ + 2e^- \rightleftarrows H_2O_2 \quad E^o = 0.68 \text{ V vs. SHE} \quad (7)$$

$$Fe^{2+} + H_2O_2 \longrightarrow Fe^{3+} + •OH + OH^- \quad (8)$$

While homogenous EF has higher efficiency than heterogeneous EF, heterogeneous EF catalysts can be reused.[139] The limiting steps are the activation of H_2O_2 and the reduction of Fe(III) to Fe(II) to complete the catalytic cycle.[140] The use of Fe as a sacrificial anode in hetero-EF catalysis can enhance its efficiency.[141] Oxidation from Fe to Fe(II) in water results in formation of H_2O_2.[142] The inclusion of a second metal, for example, Mn (Mn(II)/Mn E° = −1.18 V vs. SHE), can be used to regenerate Fe(II) ions.[143,144] For instance, a Fe/Mn based MOF linked through 1,4-phthalic acid, FeMn@C, has been used to electrochemically degrade Carbamazepine (CBZ), an antiepileptic and mood-stabilizing drug that is a common residual pharmaceutical found in water bodies. A suspension of FeMn@C-800/2 in water degrades CBZ through a hetero-EF process with a FE of 98%, a *j* of 10 mA cm^{-2} in 40 min. The degradation of the FeMn@C MOF leads to the leaching of Fe(II) that can be oxidized to Fe(III) and act as a homo-EF catalyst with a FE of 34% which suggests that the Fe/Mn@C-800/2 is responsible for the degradation activity (Fig. 4a).[145] A related Fe/Mn MOF can degrade sulfamethoxazole (SMX), a widely used antibiotic commonly found in effluents in China,[146,147] through a hetero-EF process. The electrochemical characterization of $Mn_{0.67}Fe_{0.33}$-MOF-74@CF shows a larger current response value compared to the other electrodes (Fig. 4b), suggesting higher electrochemical activity. $Mn_{0.67}Fe_{0.33}$-MOF-74@CF can degrade SMX with a 96% FE, *j* of 14 mA cm^{-2} at the optimal pH 3 conditions.[148] An Fe/Co MOF, N-Co/Fe-PC, is another hetero-EF catalyst, which when coupled with electrocoagulation, fully demetalates the metal-antibiotic complex Cu-Ciprofloxacin (CIP), which is often formed in wastewater by the Cu complexation of CIP (Fig. 4c). It can further degrade CIP with a FE of 96% *j* of 35 mA cm^{-2} in 40 min. EPR measurements suggest that $•OH$ and $•O_2^-$ are the radicals present in this degradation.[149]

MOF-derived electrodes obtained by the carbonization of $Cu(NO_3)_3 \cdot 3H_2O$ with H_3BTC (Trimesic acid) under N_2, CuOx-C-550 N, and dropcasted on stainless-steel mesh can be used for the anodic oxidation of ceftazidime (CAZ), which is an antibiotic of the β-lactam group found in wastewaters. The optimal CuOx-C-550 N electrodes degrade CAZ with a FE of 100% in 20 min. This electrode shows a decrease in efficiency of 10% over 20 cycles.[150] MOFs have the versatility of being able to test the activity of different metals while maintaining the same structural connectivity. The electrodegradation of tetracycline (TC), a widely prescribed

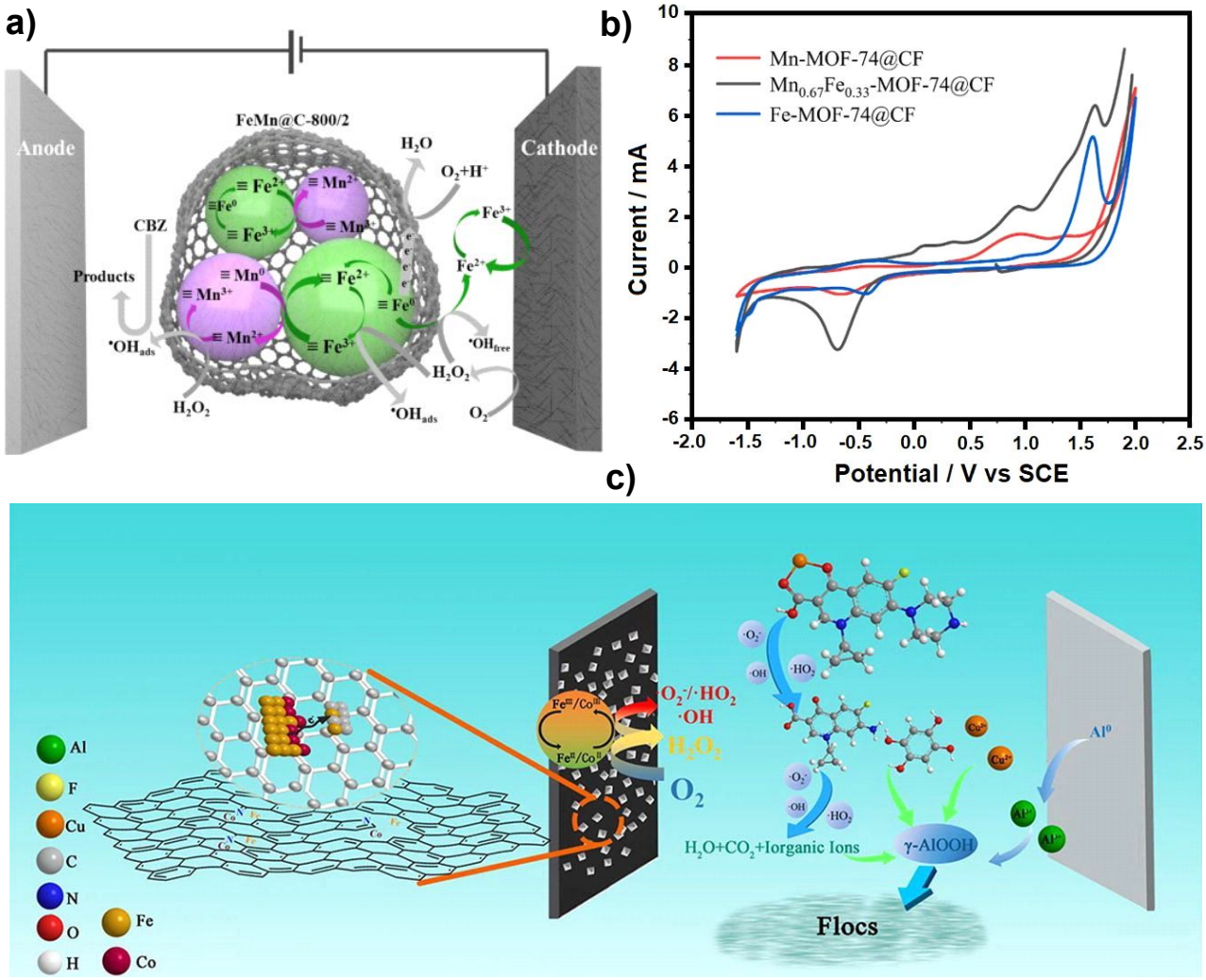

Fig. 4 (a) Proposed mechanism of the electrodegradation of carbamazepine (CBZ) by hetero-EF on FeMn@C-800/2. Reproduced with permission from ref. 145. Copyright © 2020, Elsevier. (b) Cyclic voltammogram of $Mn_{0.67}Fe_{0.33}$-MOF-74@CF and different electrodes in 0.1 M Na_2SO_4 solution, v = 10 mV s^{-1}. Reproduced with permission from ref. 148. Copyright © 2020, Elsevier. (c) Proposed mechanism for the ciprofloxacin complexes (Cu-CIP) removal by Fe/Co MOF and N-Co/Fe-PC hetero-EF catalysts. Reproduced with permission from ref. 149. Copyright © 2020, Elsevier.

antibiotic used to treat bacterial infections,[151,152] has been explored with several MOFs, namely UiO-66, MIL-100(Fe) and MIL-53(Al). Graphite supported MOFs dropcasted on Ti plates anodically degrade TC with FE of 98, 89, and 80%, respectively, at optimal conditions with *j* of 20 mA cm^{-2} on all samples. The stability of the UiO-66 electrode was measured over 6 cycles showing a decrease in activity of 8.5%.[153]

The FE of single atom nickel coordinated with nitrogen (Ni-N_4) for CO is 99% at −0.81 V vs. SHE.[154] Similarly, other types of Ni incorporated into N-doped carbon based materials, such as N-doped carbon black, Ni-nitrogenated graphene[155] and Ni-hollow carbon nanospheres,[156] show close to 99% FE for CO production at potentials ranging from −0.6 to −0.8 vs SHE. Mn-N_3- graphitic carbon nitride show outstanding potential for CO_2RR with FE of 98.8% of CO at −0.55 V vs. SHE.[157] Fe molecular systems such as Fe-porphyrin/graphene frameworks (FePGF) can electrochemically generate CO with FE of 99% at −0.54 V vs. SHE in 10 h.[158] Amino functionalized iron-tetraphenylporphyrins (amino-Fe-TPPs) can reach FE of 87% at −1.0 V vs. SHE in a flow cell with alkaline media.[159] Cu-N-doped carbon can reduce CO_2 to ethanol with FE of 55% at −1.2 V vs. SHE, while the conversion yield of C_2-products (ethanol and ethylene) is 80%.[160]

3. Degradation of Poly- and per-fluoroalkyl substances (PFAS) by homogenous catalysis

For over 60 years, perfluorinated compounds have been used in many industries for a broad range of consumer products.[161] Poly- and per-fluoroalkyl substances (PFAS) are man-made chemicals whose carbon chains are partially or completely saturated with fluorine atoms. PFAS are emergent persistent pollutants identified as a source of public health concern because of their environmental thermal and chemical stability (their half-life in water is over 90 years) and related human impact.[162–165] To date, over 4,000 PFAS have been identified. The most common are per-fluorocarboxylic (PFCAs) and perfluorosulfonic acids (PFSAs).[166,167] PFAS are well known for their hydrophobic and lipophobic properties and their stable C-F bonds.[161]

Table 1. Summary of experimental conditions and electrochemical behavior of molecular inspired electrocatalysts for degradation of pollutants.

Electrocatalyst	Pollutant	E_{app}	j_{app} [mA cm^{-2}]	Time [h]	FE	Main Product	TOF[a] [h^{-1}]	Ref.
			Nitrate/Nitrite					
$[Co(DIM)Br_2]^+$	NO_3^-	−0.80 V vs. SHE	−120	–	97%	NH_3	–	73
$[Co(TIM)Br_2]^+$	NO_2^-	−0.66V vs. SHE	−2	1	85%	NH_2OH	42	72
GCC-CoDIM	NO_2^-	−1.16 V vs. SHE	–	4	>99%	NH_3	180.9	68
GCC-FeDIM	NO_3^-	−0.86 V vs. SHE	–	4	88%	NH_3	692.3	69
NiPc-CNT	NO_3^-	−1.10 V vs. SHE	–	4	87%	NH_3	–	80
CuPc-CNT	NO_3^-	−0.55 V vs. SHE	−980	–	98%	NH_3	–	79
CoPc-CNT	NO_2^-	−0.192 V vs. SHE	−466	–	97%	NH_3	–	79
$Co(dmgH_2)Cl_2$-MWCNTs	NO_2^-	−0.34 V vs. SHE	–	1	98%	NH_3	–	82
Co_1Cu_2HHTP	NO_3^-	−0.6 V vs. SHE	−100	0.5	96%	NH_3	–	83
Cu/CuO_2/CuO-MOF	NO_3^-	−0.3 V vs. SHE	–	1	99%	NH_3	–	84
Cu@Th-BYPYDC	NO_3^-	0 V vs. SHE	–	2	93%	NH_3	–	85
Cu-MOF	NO_3^-	−0.9 V vs. SHE	–	1	85%	NH_3	–	86
Fe_3Ni-N-C	NO_3^-	−1.06 V vs. SHE	−25	0.5	52%	N_2	–	88
Ni-MOF/NF	NO_3^-	−1.16 V vs. SHE	−40	6	14%	NH_3	–	89
RuNi-MOF	NO_3^-	−1.10 V vs. SHE	–	–	73%	NH_3	–	90
Pd-NDs/Zr-MOF	NO_3^-	−1.3 V vs. SHE	−40	6	58%	NH_3	–	91
			Halogenated compounds					
CoPc/CNT	1,2-dichloroethane	−0.34 V vs. SHE	−50.0	–	~100%	Ethylene	120	22
CuT2	CH_2Cl_2	−1.40 V vs. SHE	−25.1	10	70%	CH_4	9.2	25
H2PorT8[b]	CH_2Cl_2	−1.56 V vs. SHE	−13.0	1	70%	CH_4	130.9	106
CoPor8T[b]	Alachlor	−1.16 V vs. SHE	−4.8	–	84%	DCAl[c]	32,730	29
bi-FePc	Atrazine	0.09 V vs. SHE	–	3	98%	HEIT[d]	–	107
$[Co(bpy(CH_2OH)_2)_2]^{2+}$	Alachlor	−1.00 V vs. SHE	–	0.75	95%	DCAl[c]	24,000	108
VB12	Trichloroacetic acid	–	−7.2	5	92%	Acetic acid	–	109
VB12	Tribromoacetic acid	–	−10	6	99%	Acetic acid	–	110
			Aromatic hydrocarbons					
Fe-ZSM-5	Lindane	–		8	78%	Hydracrylic acid	–	122
PD-CTF	Nitrobenzene	−0.22 V vs. SHE		–	–	Phenyl hydroxylamine	–	123
MoS_2@ZNC	Phenol	–		2	99%	$CO_2 + H_2O$	–	124
UiO-66-from ZrO_2-C/PbO_2	2,4,6-trinitrophenol	–		2.33	94 %	$CO_2 + H_2O$	–	125
CTOHH /DNA	4-MBA[e]	–		24	91%	Methoxybenzaldehyde	–	126
			Pharmaceuticals molecules					
FeMn@C-800/2	Carbamazepine	–	10.0	1	99%	$CO_2 + H_2O$	–	145
$Mn_{0.67}Fe_{0.33}$-MOF-74@DF	Sulfamethoxazole	–	14.0	1.5	96%	$CO_2 + SO_4^{2-}$	–	148
N-Co/Fe-PC	Cu-CIP[1]	–	–	0.75	96%	$CO_2 + H_2O$	–	149
CuOx-C-550 N	Ceftazidime	–	–	0.33	100%	–	–	150
Graphite-UiO-66(Zr)/Ti	Tetracycline	–	20.0	3	98%	Oxalic acid	–	153

[a] TOF: turnover frequency.
[b] The experiment was performed in acetonitrile.
[c] DCAl: dechlorinated alachlor.
[d] HEIT: 2-hydroxy-4-ethylamino-6-isopropylamino-1,3,5-triazine.
[e] 4-MBA: 4-methoxybenzyl alcohol

As a consequence of the wide usage range of PFAS, they have been found in living organisms, food, surface soils, and drinking water.[163,164,168,169] Contaminated drinking water is one of the main sources of human exposure. The current health advisory limit proposed by the Environmental Protection Agency (EPA) for perfluorooctanoic acid (PFOA), perfluorooctanoic sulfonate (PFOS), hexafluoropropylene oxide dimer acid (HFPOs or GenX), and perfluorobutane sulfonic acid (PFBS) is 0.004 ng L^{-1}, 0.020 ng L^{-1}, 5.000 ng L^{-1}, and 2,000 ng L^{-1}, respectively.[164,168,170] Therefore, there is a need to control the concentrations of PFAS in the environment with a major concern in drinking water systems. Many technologies have been used to remove PFAS from water-related environments, including adsorption, chemical oxidation, chemical reduction, biotreatment, ultrasonication, photocatalytic degradation, and electrochemical methods.[171,172] Electrochemical methods in water treatment are becoming popular due to many advantages, such as scalability, as they can be applied at the source of contamination. Electrochemical methods can also target a broad spectrum of pollutants while being easy to operate.[173–175] Currently, most of the electrochemical PFAS degradation efforts have been focused on the study of materials such as boron-doped diamond (BDD) electrodes and mixed metal oxide (MMO), and little work has been performed on molecularly inspired electrocatalytic systems.[176–181] Yet, some MOFs and molecular systems have shown potential for their PFAS removal applications.

A titanium-based MOF, MIL-125-NH2, was found to efficiently degrade 98.9 % of PFOA (100 µg L^{-1}) with a 67% defluorination rate in 24 hours through reductive photocatalysis under the irradiation of a Hg vapor lamp in the presence of glucose as the sacrificial reductant.[182] The degradation is believed to follow a chain shortening and H/F exchange path. Density functional theory (DFT) studies suggest that hydroxyl radical (•OH) is important in helping hydrated electron (e_{aq}^-) initiate the PFAS reduction. Several examples in the literature show photochemical and chemical

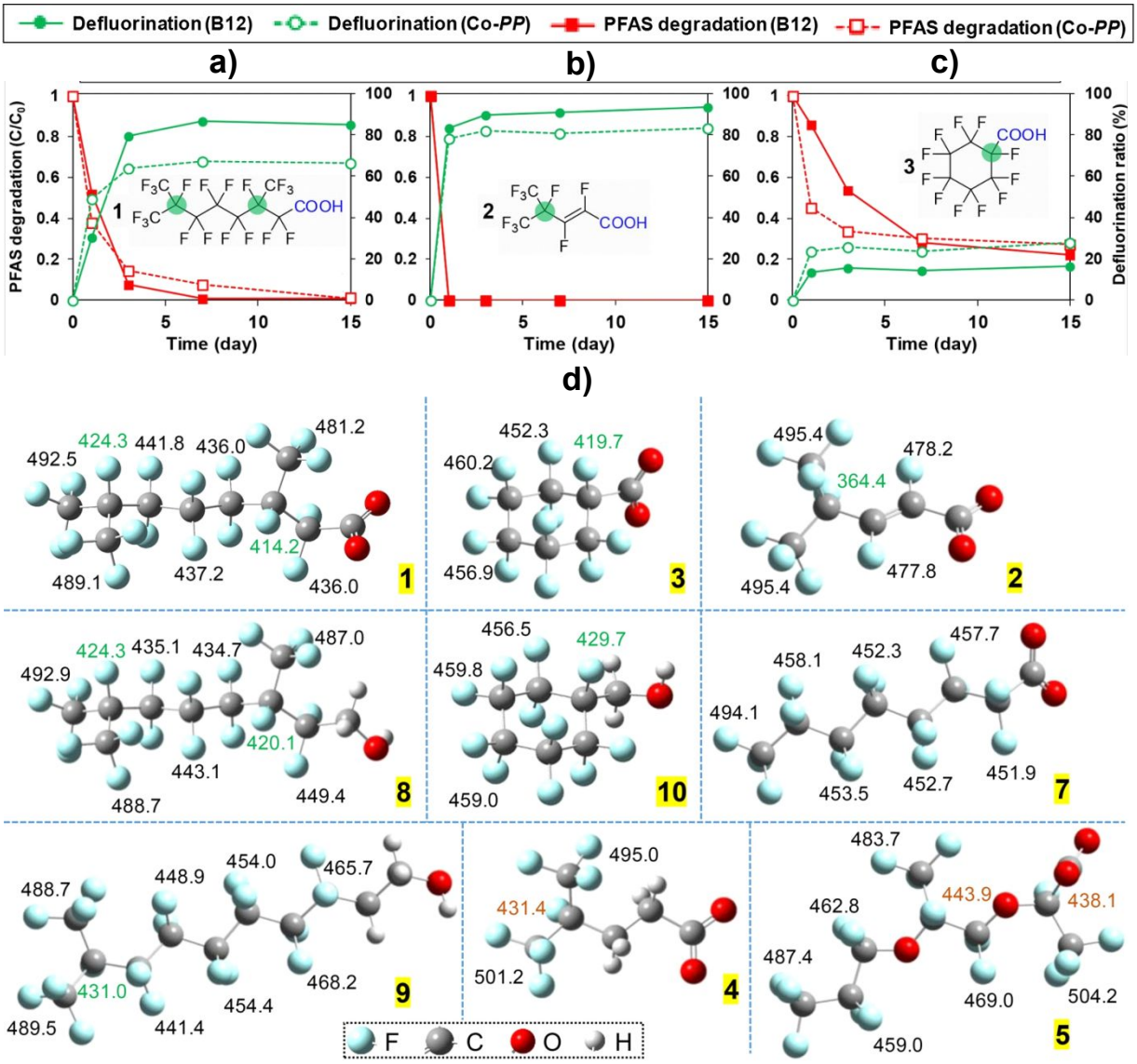

Fig. 5 Degradation and defluorination ratio of PFAS with Co(II)-porphyrin and VB12, over 15 days of catalysis. (a) perfluoro-3,7-dimethyloctanoic acid. (b) 4-(Trifluoromethyl)hexafluoropent-2-enoic acid. (c) perfluorocyclohexylcarboxylic acid. Reaction conditions: PFAS (0.1 mM), Co-catalyst (0.25 mM), Ti(III) citrate (~36 mM), and carbonate buffer (~40 mM) in water at pH 9.0, T= 70 °C. (d). Calculated bond dissociation energies (BDEs, in kJ mol^{-1}) at the B3LYP/6-311+G(2d,2p)/SMD level of theory. Reproduced with permission from ref. 188. Copyright © 2019, American Chemical Society.

reductive and oxidative processes for removing PFAS. Since none of those processes are electrochemical in nature, they are not in the purview of this article. Thus, we shall very briefly list some here. TiO_2 based materials can photocatalytically degrade PFOA under UV-Vis conditions at 100%.[178,183,184] PFAS can be chemically defluorinated with Vitamin B12,[185] or Co(II)-porphyrin and Fe(III)- porphyrins, as a catalyst and Ti(III)–citrate as a reductant.[186] Figure 5 shows the degradation efficiency and the defluorination ratio (%) of PFAS, using a Co(II)-porphyrin (Co-PP) and the mixture of Vitamin B12 with Ti(III)–citrate. As shown in Figure 5a, the 85% defluorination for the perfluoro-3,7-dimethyloctanoic acid, is achieved in 7 days. A higher defluorination ratio was obtained (92%) for the 4-(Trifluoromethyl)hexafluoropent-2-enoic acid (Fig. 5b). In both cases, 100% degradation was achieved after 15 days. The perfluorocyclohexylcarboxylic acid, results in a lower defluorination and degradation with 30% and 60%, respectively. The chemical environment around the tertiary carbon-fluorine (C-F) bond was found to be crucial for reactivity with cobalt active site. For linear PFAS with only primary and secondary carbons (as PFOA), no significant defluorination was achieved. The mechanistic aspects of each PFAS degraded were correlated with the calculated bond dissociation energies (Figure 5d), offering valuable insights into the initial defluorination steps.[187] A general proposed mechanism for reductive defluorination suggests that tertiary C-F bonds initiate the H/F exchange, with an elimination step at secondary C-F bonds. Because most of the molecularly inspired PFAS degradation studies follow a chemical reduction rather than electrochemical redox processes, we suggest that these research efforts provide a footprint for the use in the rational design of molecular-inspired electrodegradation of PFAS.[188]

4. Computational chemistry as an important tool in electrocatalysis

Computational chemistry broadly encompasses using computational methods based on classical or quantum mechanical concepts to understand chemical systems and solve chemical problems.[189] Its use has been extended to several areas (i.e., drug discovery[190,191], synthetic chemistry[192,193], environmental chemistry[194], materials science[195–197]) thanks to its cost-effective predictive power, which yields insights into the molecular behavior of molecules and materials.[198] In electrocatalysis, computational chemistry methods have been highlighted as tools to guide electrocatalyst discovery, design, and engineering since they can replace trial-and-error experiments with a rational design strategy.[199] Computational chemistry can provide reaction mechanisms, identification/characterization of active sites, surface interactions, solvent effects, binding energies, structure-property relationships, among others.[200,201]

Computational chemistry has been used to provide mechanistic details of nitrate reduction (NO_3RR).[202–204] The electronic structure of the two-dimensional nickel porphyrin-based COF electrocatalyst, NiPr-TPA-COF, suggests that Ni-3d orbitals are localized close to the Fermi level (E_F) with a considerable overlap with N-2p and C-2p orbitals; thus, inducing a fast site-to-site electron transfer from C and N sites to the Ni center. The Ni center also generates an efficient electron path for electrolysis, given that it increases the electron density near the E_F of neighboring C sites in the porphyrin scaffold. The Ni center was found to be the NO_3RR catalytic site because of orbital overlap between adsorbed NO_3* and Ni-3d orbitals and thermodynamically favorable adsorption energies of NO_3 (-0.23 eV) and H_2O (-0.11 eV). The proposed reaction path (Fig. 6a) starts with nitrate adsorption on the catalyst surface followed by dissociation to NO_2* and NO*. NO* intermediate undergo three proton-coupled electron transfers to form NH_2OH*, which is then reduced to NH_3.[202] A host-guest ultrasmall Cu nanocatalyst (1-Cu') for NO_3RR to NH_3 can be prepared *in situ* from the reconstruction of a MOF-supported single-atom Cu precatalyst (1-Cu) (Fig. 6b).[203] In contrast to other MOFs, 1-Cu does not collapse the host $[Ce_6O_4(OH)_4(BDC)_6]$ framework (Fig. 6b-1) upon 1-Cu reconstruction providing support for the ultrasmall Cu nanoclusters and avoiding aggregation. DFT calculations show that host-guest interaction between the framework and the Cu13 cluster and a strong binding affinity of the confined Cu cluster active center and NO_3^-. The host−guest interaction makes NO_3RR thermodynamically favorable. The RDS ($*NH_3$ formation) ΔG values were 0.58, 1.08, and 0.76 eV for the confined Cu13 cluster, nonconfined Cu13 cluster, and Cu(111) slab, respectively.

MXenes (Ti_3C_2Tx), composed of atomically thin 2D transition metal carbides or carbonitrides, have received significant attention for electrochemical applications given their high electrical conductivity, large surface area, and hydrophilicity.[205] The 2D flexible highly defective $Ti_3C_2T_x$ MXene exhibits selectivity for NO_3RR to N_2 at 83%.[204] DFT calculations (Fig. 6c) show that O vacancies in the MXene structure enhances NO_3^- adsorption (ΔG = −2.46 eV). After adsorption, the conversion of $*NO_3$ to N_2 is thermodynamically downhill with a maximum activation energy of 2.97 eV. The conversion of $*NO_3$ to NH_3 is less likely to occur, given the unfavorable energy barrier for $*NH_3$ desorption (0.36 eV) and the limited supply of *H.

The use of density functional theory (DFT) in electrocatalysis has also enabled researchers to explore the electrochemical degradation of other pollutants.[206–208] For example, the selective detection and Electro Fenton oxidation of PFOA were achieved using a bifunctional electrode fabricated by a modified polypyrrole molecular imprinted polymer (MIP) with an electrospun carbon nanofiber Co/Fe MOF composite (Co/Fe@CNF).[208] Independent gradient model (IGM) analyses and density functional theory calculations suggest that the nature of the binding between PFOA and Co/Fe@CNF electrode is a O–H-π hydrogen bond. The calculated distance between the carboxyl group of PFOA and the pyrrole scaffold in the MIP is 2.2 Å, which suggests that the carboxyl group inserts into the π system of the pyrrole ring. The calculated binding energy of PFOA on the MIP is 54.7 kJ mol^{-1}, indicating a strong absorption capacity of PFOA, which is a crucial step for the electrochemical degradation of the pollutant.

The removal of organic pharmaceutical pollutants, such as 2,4-dichlorophenol, naproxen, and ciprofloxacin, has been studied computationally and experimentally with an iron single-atom catalyst (Fe-SAC/NC) in heterogeneous EF.[206] DFT calculations were employed to explore the difference in activity towards H_2O_2 between the single-atom (Fe-SA/NC) and the nanoparticle (Fe-NP/NC) catalysts (Fig. 6d). Adsorption of H_2O_2 on the iron site occurs first where one of the O atoms of H_2O_2 binds to the iron site. Then, a proton is released to form a HOO* intermediate, followed by the breaking of the O-O bond to yield a HO* species. The generated *OH is rapidly desorbed from the material as •OH radical to oxidize the pollutants. The O-O breakage from HOO* to HO* is more thermodynamically favorable on Fe-SAC/NC (-3.11 eV vs. -2.76 eV). Besides, the desorption of •OH is exothermal in Fe-SAC/NC, whereas in Fe-NP/NC is endothermal, which suggests the higher EF activity of the Fe-SAC/NC over the nanoparticle analog.

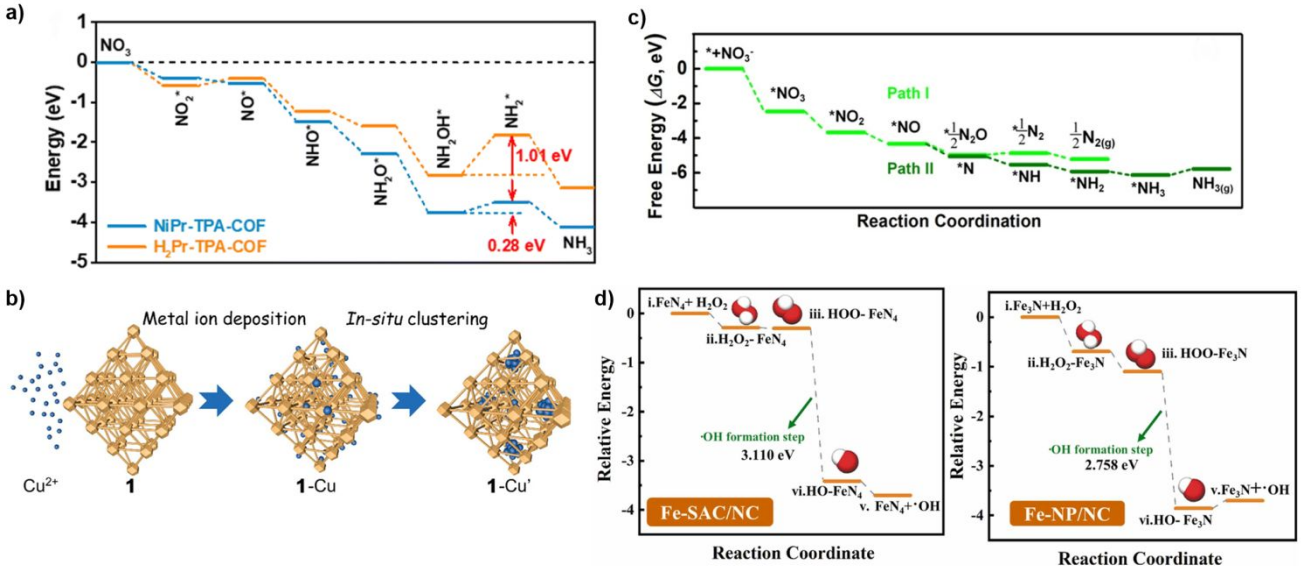

Fig. 6 (a) Gibbs free energy profile of the NO_3RR to NH_3 over NiPr-TPA-COF. Reproduced with permission from ref. 202. Copyright © 2023, Royal Society of Chemistry. (b) Schematic picture showing the reconstruction and evolution of the host–guest 1-Cu catalyst. Reproduced with permission from ref. 203. Copyright © 2022. American Chemical Society. (c) Calculated free energy reaction pathways for the conversion of nitrate to N_2 (Path I) and to NH_3 (Path II) on Ti_3C_2Tx MXene nanosheets. Reproduced with permission from ref. 204. Copyright © 2021. American Chemical Society. (d) Computed reaction profile for H_2O_2 activation at single-atom (Fe-SA/NC) and nanoparticle (Fe-NP/NC) catalysts. Reproduced with permission from ref. 206. Copyright © 2023, Elsevier.

The electrocatalytic reductive debromination of tribromoacetic acid (TBAA) using Vitamin B_{12} (VB_{12}) was studied by DFT.[209] Atomic H* was confirmed to have a prominent role in the debromination of TBAA. The calculated energy profile for H* formation starts with the adsorption of H_2O on the surface of the VB_{12}-modified electrode (-0.13 eV). The adsorbed H_2O is then activated to generate atomic H* with a relatively low energy barrier (0.61 eV) to, in turn, promote the dissociation of C-Br bonds. DFT was also employed to yield mechanistic insights into the dechlorination of CH_2Cl_2 to CH_4 mediated by a triazole-based copper (I) system (CuT2).[25] The reaction starts with the reduction of CuT2 (-1.65 eV) followed by the endothermic coordination of CH_2Cl_2 (0.13 eV). Upon coordination, the Cu site can dissociate the first C – Cl bond with a barrier of 0.15 eV. The reaction is then followed by two one-electron reductions, a protonation, and the activation/ dissociation of the second C–Cl bond (0.45 eV). A fourth one-electron reduction and a protonation step form the product CH_4 and regenerate the electrocatalyst. In another study, grand canonical quantum mechanical calculations were performed to study the dechlorination of 1,2-dichloroethane (DCA) to ethylene. The proposed mechanism has two electron-coupled dechlorination steps that yield chloroethyl ($*C_2H_4Cl$) and ethylene, respectively. The first dichlorination process is the RDS, in which the kinetic free-energy barrier decreases from 0.78 eV to 0.68 eV when the potential reduces from 0 V to −0.6 V.[22]

The examples provided herein exemplify the valuable applications of computational chemistry in environmentally relevant electrocatalytic studies utilizing molecular-inspired electrocatalysts. We recommend referring to other reviews focused specifically on this topic for a more comprehensive understanding of computational methods in electrocatalysis.[200,201,210–213]

Conclusions

In this review, we present the latest advancements in molecular-inspired electrocatalysts for degrading pollutants of public concern. These catalysts, such as metal complexes, porphyrins, phthalocyanines, and molecular-based extended networks like metal-organic frameworks (MOFs), possess physical and redox properties that enable them to undergo electrochemical reactions for pollutant degradation in water bodies. Molecular inspiration offers several advantages, including the ability to fine-tune the electrocatalyst through synthetic techniques, the need for moderate reaction conditions, and the potential for scalability. On the other hand, molecularly inspired systems have increased costs with increased volume, the stability of the catalysts must be improved, and interfering species may affect pollutant removal efficiency. Molecular electrocatalysts can mitigate the impact of highly persistent pollutants on the environment, particularly in water bodies. However, further research in this field is necessary to develop more efficient and cost-effective electrocatalysts for water remediation and address the challenges associated with their practical application.

Author Contributions

Jonathan J. Calvillo Solis contributed to the conceptualization, project administration, data curation, original draft writing, and review and editing.

Alexandria Castillo contributed to the conceptualization, data curation, original draft writing, and review and editing.

Sheng Yin contributed to the conceptualization, data curation, original draft writing, and review and editing.

Christian Sandoval Pauker contributed to the conceptualization, data curation, original draft writing, and review and editing.

Neidy D. Ocuane contributed to the conceptualization, data curation, original draft writing, and review and editing.

Diego Solis Puerto contributed to the conceptualization, data curation, original draft writing, and review and editing.

Nasim Jafari contributed to the conceptualization, data curation, original draft writing, and review and editing.

Dino Villagran contributed to the conceptualization, funding acquisition, supervision, review and editing.

Conflicts of interest

There are no conflicts to declare.

Acknowledgements

We thank NSF Nanosystems Engineering Research Center for Nanotechnology-Enabled Water Treatment (NEWT) (ERC-1449500) and the Welch Foundation under award number AH-2083-20210327 for providing financial support.

References

1 M. C. Villarín and S. Merel, *J. Hazard. Mater.*, 2020, **390**, 122139.
2 K. C. Jones, *Environ. Sci. Technol.*, 2021, **55**, 9400–9412.
3 C. Zamora-Ledezma, D. Negrete-Bolagay, F. Figueroa, E. Zamora-Ledezma, M. Ni, F. Alexis and V. H. Guerrero, *Environ. Technol. Innov.*, 2021, **22**, 101504.
4 P. Chowdhary, A. Raj and R. N. Bharagava, *Chemosphere*, 2018, **194**, 229–246.
5 N. H. H. Hairom, C. F. Soon, R. M. S. R. Mohamed, M. Morsin, N. Zainal, N. Nayan, C. Z. Zulkifli and N. H. Harun, *Environ. Technol. Innov.*, 2021, **24**, 102032.
6 Y. Vasseghian, S. Hosseinzadeh, A. Khataee and E.-N. Dragoi, *Sci. Total Environ.*, 2021, **796**, 149000.
7 J. Aravind kumar, T. Krithiga, S. Sathish, A. A. Renita, D. Prabu, S. Lokesh, R. Geetha, S. K. R. Namasivayam and M. Sillanpaa, *Sci. Total Environ.*, 2022, **831**, 154808.
8 X. Yang, W. Ou, Y. Xi, J. Chen and H. Liu, *Environ. Sci. Technol.*, 2019, **53**, 7019–7028.
9 B. Sun, Q. Li, M. Zheng, G. Su, S. Lin, M. Wu, C. Li, Q. Wang, Y. Tao, L. Dai, Y. Qin and B. Meng, *Environ. Pollut.*, 2020, **265**, 114908.
10 L. Baptista-Pires, G.-F. Norra and J. Radjenovic, *Water Res.*, 2021, **203**, 117492.
11 Y. He, D. Zhao, H. Lin, H. Huang, H. Li and Z. Guo, *Curr. Opin. Electrochem.*, 2022, **32**, 100878.
12 A. S. Mramba, P. P. Ndibewu, L. L. Sibali and K. Makgopa, *Electroanalysis*, 2020, **32**, 2615–2634.
13 D. Zhi, Y. Lin, L. Jiang, Y. Zhou, A. Huang, J. Yang and L. Luo, *J. Environ. Manage.*, 2020, **260**, 110125.
14 C. Thamaraiselvan, D. Bandyopadhyay, C. D. Powell and C. J. Arnusch, *Chem. Eng. J. Adv.*, 2021, **8**, 100195.
15 D. Clematis and M. Panizza, *Curr. Opin. Electrochem.*, 2021, **30**, 100844.
16 A. Arevalo-Bastante, S. Omar, J. Palomar, M. A. Alvarez-Montero, J. Bedia, J. J. Rodriguez and L. M. Gómez-Sainero, *Chem. Eng. J.*, 2022, **446**, 136893.
17 T. Gensch, M. N. Hopkinson, F. Glorius and J. Wencel-Delord, *Chem. Soc. Rev.*, 2016, **45**, 2900–2936.
18 D. W. Flaherty, D. D. Hibbitts and E. Iglesia, *J. Am. Chem. Soc.*, 2014, **136**, 9664–9676.
19 P. J. Moon and R. J. Lundgren, *ACS Catal.*, 2020, **10**, 1742–1753.
20 M. E. Walsh, P. Kyritsis, N. A. J. Eady, H. A. O. Hill and L.-L. Wong, *Eur. J. Biochem.*, 2000, **267**, 5815–5820.
21 A. Modak and D. Maiti, *Org. Biomol. Chem.*, 2015, **14**, 21–35.
22 C. Choi, X. Wang, S. Kwon, J. L. Hart, C. L. Rooney, N. J. Harmon, Q. P. Sam, J. J. Cha, W. A. Goddard, M. Elimelech and H. Wang, *Nat. Nanotechnol.*, 2023, **18**, 160–167.
23 X. Chen, X. Hu, L. An, N. Zhang, D. Xia, X. Zuo and X. Wang, *Electrocatalysis*, 2014, **5**, 68–74.
24 N. Devi, C. K. Williams, A. Chaturvedi and J. "Jimmy" Jiang, *ACS Appl. Energy Mater.*, 2021, **4**, 3604–3611.
25 C. K. Williams, G. A. McCarver, A. Lashgari, K. D. Vogiatzis and J. "Jimmy" Jiang, *Inorg. Chem.*, 2021, **60**, 4915–4923.
26 W. Zheng and L. Y. S. Lee, *ACS Energy Lett.*, 2021, **6**, 2838–2843.
27 N. Kaeffer and W. Leitner, *JACS Au*, 2022, **2**, 1266–1289.
28 C. K. Williams, A. Lashgari, N. Devi, M. Ang, A. Chaturvedi, P. Dhungana and J. J. Jiang, *Chem. – Eur. J.*, 2021, **27**, 6240–6246.
29 N. Devi, P. Sarkar, A. Patel and J. "Jimmy" Jiang, *ChemCatChem*, 2023, **15**, e202201512.
30 Michael J. Pennino, Jana E. Compton, and Scott G. Leibowitz, *Environ. Sci. Technol.*, 2017, **51**, 13450–13460.
31 Karen R. Burow, Bernard T. Nolan, Michael G. Rupert, and Neil M. Dubrovsky, *Environ. Sci. Technol.*, 2010, **44**, 4988–4997.
32 Michael J. Pennino, Scott G. Leibowitz, Jana E. Compton, Ryan A. Hill, and Robert D. Sabo, *Sci. Total Environment*, 2020, **722**, 137661.
33 Anna M. Fan and Valeria E. Steinberg, 1996, **23**, 35–43.
34 Mary H. Ward, Rena R. Jones, Jean D. Brender, Theo M.De Kok, Peter J. Weyer, Bernard T. Nolan, Cristina M. Villanueva, and Simone D. Van Breda, *Int. J. Environ. Res. Public Health*, 2018, **15**, 1557.
35 Nadia Espejo-Herrera, Kenneth P Cantor, Nuria Malats, Debra T. Silverman, Adonia Tardon, Reina Garcia-Closas, Consol Serra, Manolis Kogevinas, and Cristina M. Villanueva, *Environ. Res.*, 2015, **137**, 299–307.
36 WHO, 2016.
37 EPA, 2017.
38 G. Horanyi and E. M. Rizmayer, *J. Electroanal. Chem.*, 1985, **188**, 265–272.
39 Hu-lin Li, Daniell H. Robertson, James Q. Chambers, and David T. Hobbs, *J. Electrochem. Soc.*, 1988, **135**, 1154.
40 Shailesh Prasad, John W. Weidner, and Andrew E. Farell, *J. Electrochem. Soc.*, 1995, **142**, 3815.
41 J. D. Genders, D. Hartsough, and D. T. Hobbs, *J. Appl. Electrochem.*, 1996, **26**, 1–9.
42 J. O'M Bockris and J. Kim, *J. Appl. Electrochem.*, 1997, **27**, 623–634.
43 Jiefei Yu and Margret J. Kupferle, *Water Air Soil Pollut: Focus*, 2008, **8**, 379–385.
44 Xuejiao Ma, Miao Li, Chuanping Feng, and Zhen He, *J. Hazard. Mater.*, 2020, **388**, 122085.

45 Dong Xu, Yang Li, Lifeng Yin, Yangyuan Ji, Junfeng Niu, and Yanxinn Yu, *Front. Environ. Sci. Eng.*
46 Matteo Duca and Marc. T. M. Koper, *Energy Environ. Sci.*, 2012, **5**, 9726–9742.
47 Yachao Zeng, Cameron Priest, Guofeng Wang, and Gang Wu, *Small Methods*, 2020, **4**, 2000672.
48 Sergi Garcia-Segura, Mariana Lanzarini-Lopes, Kiril Hristovski, and Paul Westerhoff, *Appl. Catal. B: Environ.*, 2018, **236**, 546–568.
49 A. J. Timmons and M. D. Symes, *Chem. Soc. Rev.*, 2015, **44**, 6708–6722.
50 C. L. Ford, Y. J. Park, E. M. Matson, Z. Gordon and A. R. Fout, *Science*, 2016, **354**, 741–743.
51 Y. Li, Y. K. Go, H. Ooka, D. He, F. Jin, S. H. Kim and R. Nakamura, *Angew. Chem. Int. Ed.*, 2020, **59**, 9744–9750.
52 Y. Li, A. Yamaguchi, M. Yamamoto, K. Takai and R. Nakamura, *J. Phys. Chem. C*, 2017, **121**, 2154–2164.
53 Y. Wang and B. Zhang, *J. Energy Chem.*, 2021, **53**, 90–92.
54 Y. Guo, J. R. Stroka, B. Kandemir, C. E. Dickerson and K. L. Bren, *J. Am. Chem. Soc.*, 2018, **140**, 16888–16892.
55 G. Cioncoloni, I. Roger, P. S. Wheatley, C. Wilson, R. E. Morris, S. Sproules and M. D. Symes, *ACS Catal.*, 2018, **8**, 5070–5084.
56 Y.-L. Chang, H.-Y. Chen, S.-H. Chen, C.-L. Kao, M. Y. Chiang and S. C. N. Hsu, *Dalton Trans.*, 2022, **51**, 7715–7722.
57 M. Ghazouani, H. Akrout and L. Bousselmi, *Environ. Sci. Pollut. Res.*, 2017, **24**, 9895–9906.
58 E. Lacasa, P. Cañizares, J. Llanos and M. A. Rodrigo, *J. Hazard. Mater.*, 2012, **213–214**, 478–484.
59 O. Brylev, M. Sarrazin, L. Roué and D. Bélanger, *Electrochimica Acta*, 2007, **52**, 6237–6247.
60 S. Kuwabata, S. Uezumi, K. Tanaka and T. Tanaka, *Inorg. Chem.*, 1986, **25**, 3018–3022.
61 M. H. Barley and T. J. Meyer, *J. Am. Chem. Soc.*, 1986, **108**, 5876–5885.
62 Isato Taniguichi, Norihiro Nakashima, Kiichiro Matsushita, and Kazuo Yasukouchi, *J. Electroanal. Chem.*, 1987, **224**, 19–209.
63 H. -L. Li, J. Q. Chambers, and D. T. Hobbs, 1988, **18**, 454–458.
64 M. R. Rhodes, M. H. Barley and T. J. Meyer, *Inorg. Chem.*, 1991, **30**, 629–635.
65 S.-H. Cheng and Y. O. Su, *Inorg. Chem.*, 1994, **33**, 5847–5854.
66 N. Chebotareva and T. Nyokong, *J. Appl. Electrochem.*, 1997, **27**, 975–981.
67 C. M. Moore and N. K. Szymczak, *Chem. Sci.*, 2015, **6**, 3373–3377.
68 S. Xu, H.-Y. Kwon, D. C. Ashley, C.-H. Chen, E. Jakubikova and J. M. Smith, *Inorg. Chem.*, 2019, **58**, 9443–9451.
69 S. Xu, D. C. Ashley, H.-Y. Kwon, G. R. Ware, C.-H. Chen, Y. Losovyj, X. Gao, E. Jakubikova and J. M. Smith, *Chem. Sci.*, 2018, **9**, 4950–4958.
70 S. Partovi, Z. Xiong, K. M. Kulesa and J. M. Smith, *Inorg. Chem.*, 2022, **61**, 9034–9039.
71 H.-Y. Kwon, S. E. Braley, J. P. Madriaga, J. M. Smith and E. Jakubikova, *Dalton Trans.*, 2021, **50**, 12324–12331.
72 S. E. Braley, H.-Y. Kwon, S. Xu, E. Z. Dalton, E. Jakubikova and J. M. Smith, *Inorg. Chem.*, 2022, **61**, 12998–13006.
73 S. E. Braley, J. Xie, Y. Losovyj and J. M. Smith, *J. Am. Chem. Soc.*, 2021, **143**, 7203–7208.
74 M. Ghosh, S. E. Braley, R. Ezhov, H. Worster, J. A. Valdez-Moreira, Y. Losovyj, E. Jakubikova, Y. N. Pushkar and J. M. Smith, *J. Am. Chem. Soc.*, 2022, **144**, 17824–17831.
75 S. I. Dorovskikh, D. D. Klyamer, A. D. Fedorenko, N. B. Morozova and T. V. Basova, *Sensors*, 2022, **22**, 5780.
76 S. Lu, H. Jia, M. Hummel, Y. Wu, K. Wang, X. Qi and Z. Gu, *RSC Adv.*, 2021, **11**, 4472–4477.
77 J. Shen, Y. Y. Birdja and M. T. M. Koper, *Langmuir*, 2015, **31**, 8495–8501.
78 J. Zhang, A. B. P. Lever and W. J. Pietro, *Inorg. Chem.*, 1994, **33**, 1392–1398.
79 K. S. Rajmohan and R. Chetty, *J. Appl. Electrochem.*, 2017, **47**, 63–74.
80 Y. Li, L. Ren, Z. Li, T. Wang, Z. Wu and Z. Wang, *ACS Appl. Mater. Interfaces*, 2022, **14**, 53884–53892.
81 Z. Jiang, Y. Wang, Z. Lin, Y. Yuan, X. Zhang, Y. Tang, H. Wang, H. Li, C. Jin and Y. Liang, *Energy Environ. Sci.*, 2023, 10.1039.D2EE03502B.
82 S.-L. Meng, C. Zhang, C. Ye, J.-H. Li, S. Zhou, L. Zhu, X.-B. Li, C.-H. Tung and L.-Z. Wu, *Energy Environ. Sci.*, 2023, **16**, 1590–1596.
83 J. Liu, S. Zhao, C. Wang, B. Hu, L. He, M. Wang, Z. Zhang and M. Du, *Adv. Mater. Interfaces*, 2022, **9**, 2200913.
84 P. Liu, J. Yan, H. Huang and W. Song, *Chem. Eng. J.*, 2023, **466**, 143134.
85 M. Sun, G. Wu, L. Dai, M. Oschatz and Q. Qin, *Catal. Sci. Technol.*, 2022, **12**, 6572–6580.
86 Z. Gao, Y. Lai, Y. Tao, L. Xiao, L. Zhang and F. Luo, *ACS Cent. Sci.*, 2021, **7**, 1066–1072.
87 Y.-T. Xu, M.-Y. Xie, H. Zhong and Y. Cao, *ACS Catal.*, 2022, **12**, 8698–8706.
88 J. Sun, W. Gao, H. Fei and G. Zhao, *Appl. Catal. B Environ.*, 2022, **301**, 120829.
89 F. Pan, J. Zhou, T. Wang, Y. Zhu, H. Ma, J. Niu and C. Wang, *J. Colloid Interface Sci.*, 2023, **638**, 26–38.
90 J. Qin, K. Wu, L. Chen, X. Wang, Q. Zhao, B. Liu and Z. Ye, *J. Mater. Chem. A*, 2022, **10**, 3963–3969.
91 M. Jiang, J. Su, X. Song, P. Zhang, M. Zhu, L. Qin, Z. Tie, J.-L. Zuo and Z. Jin, *Nano Lett.*, 2022, **22**, 2529–2537.
92 K. Vorkamp, J. Balmer, H. Hung, R. J. Letcher, F. F. Rigét and C. A. de Wit, *Emerg. Contam.*, 2019, **5**, 179–200.
93 C. Choi, X. Wang, S. Kwon, J. L. Hart, C. L. Rooney, N. J. Harmon, Q. P. Sam, J. J. Cha, W. A. Goddard, M. Elimelech and H. Wang, *Nat. Nanotechnol.*, 2023, **18**, 160–167.
94 Y.-Y. Lou, J.-M. Fontmorin, A. Amrane, F. Fourcade and F. Geneste, *Electrochimica Acta*, 2021, **377**, 138039.
95 B. D. Rodan, D. W. Pennington, N. Eckley and R. S. Boethling, *Environ. Sci. Technol.*, 1999, **33**, 3482–3488.
96 M. A. La Merrill, C. L. Johnson, M. T. Smith, N. R. Kandula, A. Macherone, K. D. Pennell and A. M. Kanaya, *Environ. Sci. Technol.*, 2019, **53**, 13906–13918.
97 M. Zhang, Q. Shi, X. Song, H. Wang and Z. Bian, *Environ. Sci. Pollut. Res.*, 2019, **26**, 10457–10486.
98 M. Long, J. Donoso, M. Bhati, W. C. Elias, K. Heck, Y.-H. Luo, Y. Sean Lai, H. Gu, T. Senftle, C. Zhou, M. Wong and B. Rittmann, *Environ. Sci. Technol.*, 2021, **55**, 14836–14843.
99 V. I. Kovalchuk and J. L. d'Itri, *Appl. Catal. Gen.*, 2004, **271**, 13–25.
100 E. T. Martin, C. M. McGuire, M. S. Mubarak and D. G. Peters, *Chem. Rev.*, 2016, **116**, 15198–15234.
101 K.-H. van Pée and S. Unversucht, *Chemosphere*, 2003, **52**, 299–312.
102 Z. Chen, Y. Liu, W. Wei and B.-J. Ni, *Environ. Sci. Nano*, 2019, **6**, 2332–2366.
103 R. Liu, H. Zhao, X. Zhao, Z. He, Y. Lai, W. Shan, D. Bekana, G. Li and J. Liu, *Environ. Sci. Technol.*, 2018, **52**, 9992–10002.
104 D. Huang, D. J. Kim, K. Rigby, X. Zhou, X. Wu, A. Meese, J. Niu, E. Stavitski and J.-H. Kim, *Environ. Sci. Technol.*, 2021, **55**, 13306–13316.
105 K. K. Rudman, B. Thapa, A. Tapash, M. S. Mubarak, K. Raghavachari, S. Hosseini and S. D. Minteer, *J. Electrochem. Soc.*, 2022, **169**, 115502.
106 C. K. Williams, A. Lashgari, N. Devi, M. Ang, A. Chaturvedi, P. Dhungana and J. J. Jiang, *Chem. – Eur. J.*, 2021, **27**, 6240–6246.

107 X. Chen, X. Hu, L. An, N. Zhang, D. Xia, X. Zuo and X. Wang, *Electrocatalysis*, 2014, **5**, 68–74.
108 W. He, J.-M. Fontmorin, I. Soutrel, D. Floner, F. Fourcade, A. Amrane and F. Geneste, *Mol. Catal.*, 2017, **432**, 8–14.
109 X. Ma, S. Huang, Y. Jin, H. Jiang, L. Tang, Y. Wu, Y. Ni, S. Zhu, X. Li and A. M. Dietrich, *J. Environ. Chem. Eng.*, 2023, **11**, 109944.
110 L. Wang, H. Wang, J. Deng, J. Liu, Y. Wu, S. Huang, X. Ma, X. Li and A. M. Dietrich, *J. Hazard. Mater.*, 2023, **449**, 131052.
111 A. I. Boldyrev and L.-S. Wang, *Chem. Rev.*, 2005, **105**, 3716–3757.
112 J. Aihara, *Sci. Am.*, 1992, **266**, 62–69.
113 M. E. Machado, M. M. Nascimento, P. V. Bomfim Bahia, S. T. Martinez and J. Bittencourt de Andrade, *TrAC Trends Anal. Chem.*, 2022, **150**, 116586.
114 A. Mojiri, J. L. Zhou, A. Ohashi, N. Ozaki and T. Kindaichi, *Sci. Total Environ.*, 2019, **696**, 133971.
115 O. US EPA, Relative Potency Factors for Carcinogenic Polycyclic Aromatic Hydrocarbons (PAHs), https://www.epa.gov/risk/relative-potency-factors-carcinogenic-polycyclic-aromatic-hydrocarbons-pahs, (accessed May 17, 2023).
116 M. Á. Arellano-González, I. González and A.-C. Texier, *J. Hazard. Mater.*, 2016, **314**, 181–187.
117 M. Vijayanand, A. Ramakrishnan, R. Subramanian, P. K. Issac, M. Nasr, K. S. Khoo, R. Rajagopal, B. Greff, N. I. Wan Azelee, B.-H. Jeon, S. W. Chang and B. Ravindran, *Environ. Res.*, 2023, **227**, 115716.
118 J. Muñoz, Á. Campos-Lendinez, N. Crivillers and M. Mas-Torrent, *ACS Appl. Mater. Interfaces*, 2020, **12**, 26688–26693.
119 M. Cvetnic, D. Juretic Perisic, M. Kovacic, S. Ukic, T. Bolanca, B. Rasulev, H. Kusic and A. Loncaric Bozic, *Ecotoxicol. Environ. Saf.*, 2019, **169**, 918–927.
120 Z. Hasan and S. H. Jhung, *J. Hazard. Mater.*, 2015, **283**, 329–339.
121 S. Khan, M. Sohail, C. Han, J. A. Khan, H. M. Khan and D. D. Dionysiou, *J. Hazard. Mater.*, 2021, **402**, 123558.
122 Y. Li, Y. Liu, X. Zhang, K. Tian, D. Tan, X. Song, P. Wang, Q. Jiang and J. Lu, *ACS Omega*, 2022, **7**, 33500–33510.
123 S. Gopi and M. Kathiresan, *Polymer*, 2017, **109**, 315–320.
124 L. Fan, Y. Gong, J. Wan, Y. Wei, H. Shi and C. Liu, *Chemosphere*, 2022, **298**, 134315.
125 M. Xu, J. Wang, X. Liang, W. Fang, C. Zhu and F. Wang, *Sep. Purif. Technol.*, 2023, 123921.
126 S. Kumaravel, P. Thiruvengetam, S. R. Ede, K. Karthick, S. Anantharaj, S. S. Sankar and S. Kundu, *Dalton Trans.*, 2019, **48**, 17117–17131.
127 N. Taoufik, W. Boumya, M. Achak, M. Sillanpää and N. Barka, *J. Environ. Manage.*, 2021, **288**, 112404.
128 M. Patel, R. Kumar, K. Kishor, T. Mlsna, C. U. Jr. Pittman and D. Mohan, *Chem. Rev.*, 2019, **119**, 3510–3673.
129 A. Ayati, B. Tanhaei, H. Beiki, P. Krivoshapkin, E. Krivoshapkina and C. Tracey, *Chemosphere*, 2023, **323**, 138241.
130 D. Kanakaraju, B. D. Glass and M. Oelgemöller, *J. Environ. Manage.*, 2018, **219**, 189–207.
131 A. Bhuyan and Md. Ahmaruzzaman, *Environ. Sci. Pollut. Res.*, 2023, **30**, 39377–39417.
132 I. Mohiuddin, A. L. Berhanu, A. K. Malik, J. S. Aulakh, J. Lee and K.-H. Kim, *Environ. Res.*, 2019, **176**, 108580.
133 L. Yin, B. Wang, H. Yuan, S. Deng, J. Huang, Y. Wang and G. Yu, *Emerg. Contam.*, 2017, **3**, 69–75.
134 J. Roberts, A. Kumar, J. Du, C. Hepplewhite, D. J. Ellis, A. G. Christy and S. G. Beavis, *Sci. Total Environ.*, 2016, **541**, 1625–1637.
135 A. Kumar, A. Rana, G. Sharma, Mu. Naushad, P. Dhiman, A. Kumari and F. J. Stadler, *J. Mol. Liq.*, 2019, **290**, 111177.
136 G. V. Aguirre-Martínez, C. André, F. Gagné and L. M. Martín-Díaz, *Ecotoxicol. Environ. Saf.*, 2018, **148**, 652–663.
137 R. S. Monisha, R. L. Mani, B. Sivaprakash, N. Rajamohan and D.-V. N. Vo, *Environ. Chem. Lett.*, 2022, **20**, 681–704.
138 G. Song, M. Zhou, X. Du, P. Su and J. Guo, *ACS EST Water*, 2021, **1**, 1637–1647.
139 X. Du, W. Fu, P. Su, L. Su, Q. Zhang, J. Cai and M. Zhou, *ACS EST Eng.*, 2021, **1**, 1311–1322.
140 H.-C. Li, X.-Y. Ji, X.-Q. Pan, C. Liu and W.-J. Liu, *ACS EST Eng.*, 2021, **1**, 21–31.
141 Y. Pan, Y. Zhang, M. Zhou, J. Cai and Y. Tian, *Water Res.*, 2019, **153**, 144–159.
142 H. Cheng, W. Xu, J. Liu, H. Wang, Y. He and G. Chen, *J. Hazard. Mater.*, 2007, **146**, 385–392.
143 B. Li, Z.-Y. Yan, X.-N. Liu, C. Tang, J. Zhou, X.-Y. Wu, P. Wei, H.-H. Jia and X.-Y. Yong, *Chemosphere*, 2019, **234**, 260–268.
144 X. Du, S. Wang, F. Ye and Z. Qingrui, *Environ. Res.*, 2022, **206**, 112414.
145 Y. Zheng, X. Du, G. Song, J. Gu, J. Guo and M. Zhou, *Chemosphere*, 2023, **312**, 137353.
146 W.-Q. Guo, R.-L. Yin, X.-J. Zhou, J.-S. Du, H.-O. Cao, S.-S. Yang and N.-Q. Ren, *Ultrason. Sonochem.*, 2015, **22**, 182–187.
147 Y. Zhang, B. Wang, G. Cagnetta, L. Duan, J. Yang, S. Deng, J. Huang, Y. Wang and G. Yu, *Water Res.*, 2018, **140**, 291–300.
148 D. Wu, T. Hua, S. Han, X. Lan, J. Cheng, W. Wen and Y. Hu, *Chemosphere*, 2023, **327**, 138514.
149 C. Sun, J. Wang, C. Gu, C. Wang, S. Sun and P. Song, *Chem. Eng. J.*, 2023, **452**, 139592.
150 P. Huang, J. Lei, Z. Sun and X. Hu, *Chemosphere*, 2021, **268**, 129157.
151 S. Xin, S. Huo, C. Zhang, X. Ma, W. Liu, Y. Xin and M. Gao, *Appl. Catal. B Environ.*, 2022, **305**, 121024.
152 C. Fang, S. Wang, H. Xu and Q. Huang, *Sci. Total Environ.*, 2022, **812**, 152455.
153 B. Jiang, F. Liu, Y. Pan, Y. Tan, C. Shuang and A. Li, *PLOS ONE*, 2022, **17**, e0271075.
154 X. Li, W. Bi, M. Chen, Y. Sun, H. Ju, W. Yan, J. Zhu, X. Wu, W. Chu and C. Wu, *J. Am. Chem. Soc.*, 2017, **139**, 14889–14892.
155 H. B. Yang, S.-F. Hung, S. Liu, K. Yuan, S. Miao, L. Zhang, X. Huang, H.-Y. Wang, W. Cai and R. Chen, *Nat. Energy*, 2018, **3**, 140–147.
156 C.-Z. Yuan, L.-Y. Zhan, S.-J. Liu, F. Chen, H. Lin, X.-L. Wu and J. Chen, *Inorg. Chem. Front.*, 2020, **7**, 1719–1725.
157 J. Feng, H. Gao, L. Zheng, Z. Chen, S. Zeng, C. Jiang, H. Dong, L. Liu, S. Zhang and X. Zhang, *Nat. Commun.*, 2020, **11**, 4341.
158 J. Choi, P. Wagner, R. Jalili, J. Kim, D. R. MacFarlane, G. G. Wallace and D. L. Officer, *Adv. Energy Mater.*, 2018, **8**, 1801280.
159 M. Abdinejad, C. Dao, X.-A. Zhang and H. B. Kraatz, *J. Energy Chem.*, 2021, **58**, 162–169.
160 D. Karapinar, N. T. Huan, N. Ranjbar Sahraie, J. Li, D. Wakerley, N. Touati, S. Zanna, D. Taverna, L. H. Galvão Tizei and A. Zitolo, *Angew. Chem. Int. Ed.*, 2019, **58**, 15098–15103.
161 R. C. Buck, J. Franklin, U. Berger, J. M. Conder, I. T. Cousins, P. De Voogt, A. A. Jensen, K. Kannan, S. A. Mabury and S. P. Van Leeuwen, *Integr. Environ. Assess. Manag.*, 2011, **7**, 513–541.
162 J. Glüge, M. Scheringer, I. T. Cousins, J. C. DeWitt, G. Goldenman, D. Herzke, R. Lohmann, C. A. Ng, X. Trier and Z. Wang, *Environ. Sci. Process. Impacts*, 2020, **22**, 2345–2373.
163 E. M. Sunderland, X. C. Hu, C. Dassuncao, A. K. Tokranov, C. C. Wagner and J. G. Allen, *J. Expo. Sci. Environ. Epidemiol.*, 2019, **29**, 131–147.
164 S. Yin and D. Villagrán, *Sci. Total Environ.*, 2022, **831**, 154939.

165 J. L. Domingo and M. Nadal, *Environ. Res.*, 2019, **177**, 108648.
166 OECD (The Organisation for Economic Co-operation and Development). Toward a New Comprehensive Global Database of Per- and Polyfluoroalkyl Substances (PFASs): Summary Report on Updating the OECD 2007 List of Per and Polyfluoroalkyl Substances (PFASs).
167 P. Grandjean and R. Clapp, *NEW Solut. J. Environ. Occup. Health Policy*, 2015, **25**, 147–163.
168 B. C. Crone, T. F. Speth, D. G. Wahman, S. J. Smith, G. Abulikemu, E. J. Kleiner and J. G. Pressman, *Crit. Rev. Environ. Sci. Technol.*, 2019, **49**, 2359–2396.
169 K. Rankin, S. A. Mabury, T. M. Jenkins and J. W. Washington, *Chemosphere*, 2016, **161**, 333–341.
170 J. A. Cotruvo, *J. AWWA*, 2022, **114**, 68–70.
171 K. H. Kucharzyk, R. Darlington, M. Benotti, R. Deeb and E. Hawley, *J. Environ. Manage.*, 2017, **204**, 757–764.
172 P. M. Dombrowski, P. Kakarla, W. Caldicott, Y. Chin, V. Sadeghi, D. Bogdan, F. Barajas-Rodriguez and S.-Y. D. Chiang, *Remediat. J.*, 2018, **28**, 135–150.
173 G. G. Botte, *Electrochem. Soc. Interface*, 2017, **26**, 53–61.
174 X. Li, *Int. J. Electrochem. Sci.*, 2022, ArticleID:2212110.
175 T. Muddemann, D. Haupt, M. Sievers and U. Kunz, *ChemBioEng Rev.*, 2019, **6**, 142–156.
176 J. N. Uwayezu, I. Carabante, T. Lejon, P. Van Hees, P. Karlsson, P. Hollman and J. Kumpiene, *J. Environ. Manage.*, 2021, **290**, 112573.
177 N. E. Pica, J. Funkhouser, Y. Yin, Z. Zhang, D. M. Ceres, T. Tong and J. Blotevogel, *Environ. Sci. Technol.*, 2019, **53**, 12602–12609.
178 B. Gomez-Ruiz, S. Gómez-Lavín, N. Diban, V. Boiteux, A. Colin, X. Dauchy and A. Urtiaga, *Chem. Eng. J.*, 2017, **322**, 196–204.
179 C. E. Schaefer, C. Andaya, A. Urtiaga, E. R. McKenzie and C. P. Higgins, *J. Hazard. Mater.*, 2015, **295**, 170–175.
180 B. Yang, C. Jiang, G. Yu, Q. Zhuo, S. Deng, J. Wu and H. Zhang, *J. Hazard. Mater.*, 2015, **299**, 417–424.
181 Q. Zhuo, M. Luo, Q. Guo, G. Yu, S. Deng, Z. Xu, B. Yang and X. Liang, *Electrochimica Acta*, 2016, **213**, 358–367.
182 Y. Wen, Á. Rentería-Gómez, G. S. Day, M. F. Smith, T.-H. Yan, R. O. K. Ozdemir, O. Gutierrez, V. K. Sharma, X. Ma and H.-C. Zhou, *J. Am. Chem. Soc.*, 2022, **144**, 11840–11850.
183 B. Xu, M. B. Ahmed, J. L. Zhou and A. Altaee, *Chemosphere*, 2020, **243**, 125366.
184 M. J. Rivero, P. Ribao, B. Gomez-Ruiz, A. Urtiaga and I. Ortiz, *Sep. Purif. Technol.*, 2020, **240**, 116637.
185 V. Ochoa-Herrera, R. Sierra-Alvarez, A. Somogyi, N. E. Jacobsen, V. H. Wysocki and J. A. Field, *Environ. Sci. Technol.*, 2008, **42**, 3260–3264.
186 J. Sun, S. Jennepalli, M. Lee, A. Jones, D. M. O'Carroll, M. J. Manefield, M. Bhadbhade, B. Åkermark, B. Das and N. Kumar, *Environ. Sci. Technol.*, 2022, **56**, 7830–7839.
187 J. Liu, D. J. Van Hoomissen, T. Liu, A. Maizel, X. Huo, S. R. Fernández, C. Ren, X. Xiao, Y. Fang, C. E. Schaefer, C. P. Higgins, S. Vyas and T. J. Strathmann, *Environ. Sci. Technol. Lett.*, 2018, **5**, 289–294.
188 Y. Yu, K. Zhang, Z. Li, C. Ren, J. Chen, Y.-H. Lin, J. Liu and Y. Men, *Environ. Sci. Technol.*, 2020, **54**, 14393–14402.
189 J. B. Foresman and Ae. Frisch, *Exploring chemistry with electronic structure methods*, Gaussian, Inc, Wallingford, CT, Third edition., 2015.
190 Y. Lam, Y. Abramov, R. S. Ananthula, J. M. Elward, L. R. Hilden, S. O. Nilsson Lill, P.-O. Norrby, A. Ramirez, E. C. Sherer, J. Mustakis and G. J. Tanoury, *Org. Process Res. Dev.*, 2020, **24**, 1496–1507.
191 C. N. Cavasotto, M. G. Aucar and N. S. Adler, *Int. J. Quantum Chem.*, 2019, **119**, e25678.
192 M. Elkin and T. R. Newhouse, *Chem. Soc. Rev.*, 2018, **47**, 7830–7844.
193 Q. N. N. Nguyen and D. J. Tantillo, *Chem. - Asian J.*, 2014, **9**, 674–680.
194 L. He, L. Bai, D. D. Dionysiou, Z. Wei, R. Spinney, C. Chu, Z. Lin and R. Xiao, *Chem. Eng. J.*, 2021, **426**, 131810.
195 G. Gryn'ova, K.-H. Lin and C. Corminboeuf, *J. Am. Chem. Soc.*, 2018, **140**, 16370–16386.
196 P. G. Boyd, Y. Lee and B. Smit, *Nat. Rev. Mater.*, 2017, **2**, 17037.
197 M. C. Valero and P. Raybaud, *J. Catal.*, 2020, **391**, 539–547.
198 N. Zhang, B. Yang, K. Liu, H. Li, G. Chen, X. Qiu, W. Li, J. Hu, J. Fu, Y. Jiang, M. Liu and J. Ye, *Small Methods*, 2021, **5**, 2100987.
199 G. A. Cerrón-Calle, T. P. Senftle and S. Garcia-Segura, *Curr. Opin. Electrochem.*, 2022, **35**, 101062.
200 X. Liao, R. Lu, L. Xia, Q. Liu, H. Wang, K. Zhao, Z. Wang and Y. Zhao, *ENERGY Environ. Mater.*, 2022, **5**, 157–185.
201 H. Mai, T. C. Le, D. Chen, D. A. Winkler and R. A. Caruso, *Chem. Rev.*, 2022, **122**, 13478–13515.
202 F. Lv, M. Sun, Y. Hu, J. Xu, W. Huang, N. Han, B. Huang and Y. Li, *Energy Environ. Sci.*, 2023, **16**, 201–209.
203 Y.-T. Xu, M.-Y. Xie, H. Zhong and Y. Cao, *ACS Catal.*, 2022, **12**, 8698–8706.
204 Y. Li, J. Ma, T. D. Waite, M. R. Hoffmann and Z. Wang, *Environ. Sci. Technol.*, 2021, **55**, 10695–10703.
205 M. Naguib, M. W. Barsoum and Y. Gogotsi, *Adv. Mater.*, 2021, **33**, 2103393.
206 P. Xia, Z. Ye, L. Zhao, Q. Xue, S. Lanzalaco, Q. He, X. Qi and I. Sirés, *Appl. Catal. B Environ.*, 2023, **322**, 122116.
207 X. Yang, J. Hu, L. Wu, H. Hou, S. Liang and J. Yang, *Environ. Pollut.*, 2022, **313**, 120097.
208 Y. Wang, R. Ren, F. Chen, L. Jing, Z. Tian, Z. Li, J. Wang and C. Hou, *Sep. Purif. Technol.*, 2023, **310**, 123257.
209 L. Wang, H. Wang, J. Deng, J. Liu, Y. Wu, S. Huang, X. Ma, X. Li and A. M. Dietrich, *J. Hazard. Mater.*, 2023, **449**, 131052.
210 Q. Li, Y. Ouyang, S. Lu, X. Bai, Y. Zhang, L. Shi, C. Ling and J. Wang, *Chem. Commun.*, 2020, **56**, 9937–9949.
211 N. Abidi, K. R. G. Lim, Z. W. Seh and S. N. Steinmann, *WIREs Comput. Mol. Sci.*, 2021, **11**, e1499.
212 L. M. Azofra, *Curr. Opin. Electrochem.*, 2022, **35**, 101073.
213 X. Zhang, Y. Tian, L. Chen, X. Hu and Z. Zhou, *J. Phys. Chem. Lett.*, 2022, **13**, 7920–7930.